2012

Resonance and double negative behavior in metamaterials

Yue Chen
Louisiana State University and Agricultural and Mechanical College, dickchenyue@gmail.com

RESONANCE AND DOUBLE NEGATIVE BEHAVIOR IN METAMATERIALS

A Dissertation

Submitted to the Graduate Faculty of the
Louisiana State University and
Agricultural and Mechanical College
in partial fulfillment of the
requirements for the degree of
Doctor of Philosophy

in

The Department of Mathematics

by
Yue Chen
B.S. in Math., Shanghai University, 2001
M.S. in Math, Louisiana State University, 2008
August 2012

Acknowledgments

I am sincerely and heartily grateful to my advisor, Dr. Robert Lipton, for his excellent guidance, caring, patience, and providing me with an excellent atmosphere for doing research. I would never have been able to finish my dissertation without his help. Thank Dr. Stephen Shipman, Dr. Jimmie Lawson, Dr. William Adkins, Dr. Richard A. Litherland and Dr. Ramachandra Devireddy for being on my committee.

Besides I would like to thank to my wife Wen. Her support, quiet patience and unwavering love were the bedrock upon which the past six years of my life have been built. Thank my parents for their encouragement and faith in me.

Table of Contents

Abstract

In this work, a generic class of metamaterials is introduced and is shown to exhibit frequency dependent double negative effective properties. We develop a rigorous method for calculating the frequency intervals where either double negative or double positive effective properties appear and show how these intervals imply the existence of propagating Bloch waves inside sub-wavelength structures. The branches of the dispersion relation associated with Bloch modes are shown to be explicitly determined by the Dirichlet spectrum of the high dielectric phase and the generalized electrostatic spectra of the complement. For numerical purposes, we consider a metamaterial constructed from a sub-wavelength periodic array of coated rods. Explicit power series are developed for the dispersion relation and associated Bloch wave solutions. The expansion parameter is the ratio of the length scale of the periodic lattice to the wavelength. We make use of the method of Rayleigh to numerically calculate the generalized electrostatic resonances. We apply these resonances together with the Dirichlet resonances of the core material to calculate the branches of the dispersion relation to leading order. We compare the leading order dispersion relations to the dispersion relations obtained by direct numerical simulation. These calculations show that the leading order dispersion relations is a good predictor of the dispersive behavior of the metamaterial.

Chapter 1
Introduction

1.1 History

Metamaterials are artificial materials designed to have electromagnetic properties not generally found in nature. The novelty is that unconventional electromagnetic properties can be created by carefully chosen sub-wavelength configurations of conventional materials. The distinctive properties of metamaterials are derived from geometrically induced resonances localized to specific frequencies. These resonances are used to control propagating modes with wavelengths longer than the characteristic length scale of the material. One contemporary area of research explores novel sub-wavelength constructions that deliver metamaterials with both negative bulk dielectric constant and bulk magnetic permeability across certain frequency intervals. These double negative materials are promising materials for the creation of negative index super lenses that overcome the small diffraction limit and have great potential in applications such as biomedical imaging, optical lithography and data storage.

A generic metamaterial comes most often in the form of a crystal made from a periodic array of scatterers embedded within a host medium. The physical notions of frequency dependent effective magnetic permeability and dielectric permittivity are used to describe the behavior of propagating modes at wavelengths larger than the length scale of the metamaterial crystal. The early work of Veselago [46] identified novel effects associated with hypothetical materials for which both the dielectric constant and magnetic permeability are simultaneously negative. Such double negative media support electromagnetic wave propagation in which the

phase velocity is antiparallel to the direction of energy flow, and other unusual electromagnetic effects such as the reversal of the Doppler effect and Cerenkov radiation. The double negative media remained obscure for more than three decades because no such materials exist in nature. But everything has changed since the end of last century. In 1998, Pendry [34] demonstrated that unconventional properties can be derived from subwavelength configurations of different conventional materials and showed that a cubic lattice of metal wires exhibits behavior associated with negative bulk dielectric constant. Subsequently it was shown that a periodic array of non-magnetic metallic split-ring resonators deliver negative effective magnetic permeability at microwave frequencies [35]. In more recent work, Smith et al. [44] experimentally demonstrated that metamaterials made from arrays of metallic posts and split ring resonators generate an effective negative refractive index at microwave frequencies. Building on this, Shelby et al. [41] experimentally confirmed that a microwave beam would undergo negative refraction at the interface between such a metamaterial and air. Subsequent work has delivered several new designs using different configurations of metallic resonators for double negative behavior [14, 23, 40, 51, 52, 54].

Current state of the art metallic resonators do not perform well at optical frequencies and alternate strategies are contemplated employing the use of both metals and dielectric materials for optical frequencies [39]. For higher frequencies in the infrared and optical range, new strategies for generating materials with double negative bulk properties rely on Mie resonances. One scheme employs coated rods made from a high dielectric core coated with a frequency dependent dielectric plasmonic or Drude type behavior at optical frequencies [48, 49, 50]. A second scheme employs small rods or particles made from dielectric materials with large permittivity [24, 36, 47]. Alternate strategies for generating negative bulk dielectric

permeability at infrared and optical frequencies use special configurations of plasmonic nanoparticles [1], [43]. The list of metamaterial systems is rapidly growing and comprehensive reviews of the subject can be found in [38] and [39].

1.2 Setup and outline

Despite the large number of physically based strategies for generating unconventional properties the theory lacks mathematical frameworks that:

1. Provide the explicit relationship connecting the leading order influence of double negative behavior to the existence of Bloch wave modes inside metamaterials.

2. Provide a systematic identification of the underlying spectral problems related to the crystal geometry that control the location of stop bands and propagation bands for metamaterial crystals.

In this article, we provide such a framework for a generic class of metamaterial crystals made from non-magnetic constituents. We start with a metamaterial crystal characterized by a period cell containing two parallel infinitely long cylindrical rods; one of which possesses a large frequency independent dielectric constant while the other is characterized by a frequency dependent dielectric response. In this treatment the frequency dependent dielectric response ϵ_P is associated with plasmonic or Drude behavior at optical frequencies given by [48], [49]

$$\epsilon_P(\omega) = 1 - \frac{\omega_p^2}{\omega^2}, \tag{1.2.1}$$

where ω is the frequency and ω_p is the plasma frequency [6]. The rods are parallel to the x_3 axis and are periodically arranged within a square lattice over the transverse $\mathbf{x} = (x_1, x_2)$ plane. The period of the lattice is denoted by d. There is no constraint placed on the shape of the rod cross sections other than they have

smooth boundaries and are simply connected. The objective is to characterize the branches of the dispersion relation for for H-polarized Bloch-waves inside the crystal. For this case the magnetic field is aligned with the rods and the electric field lies in the transverse plane. The direction of propagation is described by the unit vector $\hat{\kappa} = (\kappa_1, \kappa_2)$ and $k = 2\pi/\lambda$ is the wave number for a wave of length λ and the fields are of the form

$$H_3 = H_3(\mathbf{x})e^{i(k\hat{\kappa}\cdot\mathbf{x}-t\omega/c)},\ E_1 = E_1(\mathbf{x})e^{i(k\hat{\kappa}\cdot\mathbf{x}-t\omega/c)},\ E_2 = E_2(\mathbf{x})e^{i(k\hat{\kappa}\cdot\mathbf{x}-t\omega/c)} \quad (1.2.2)$$

where $H_3(\mathbf{x})$, $E_1(\mathbf{x})$, and $E_2(\mathbf{x})$ are d-periodic for $\mathbf{x}$ in $\mathbb{R}^2$. Here c denotes the speed of light in free space. We denote the unit vector pointing along the x_3 direction by $\mathbf{e}_3$, and the periodic dielectric permittivity and magnetic permeability are denoted by a_d and μ respectively. The electric field component $\mathbf{E} = (E_1, E_2)$ of the wave is determined by

$$\mathbf{E} = -\frac{ic}{\omega a_d}\mathbf{e}_3 \times \nabla H_3. \quad (1.2.3)$$

The materials are assumed non-magnetic hence the magnetic permeability μ is set to unity inside the rods and host. The oscillating dielectric permittivity for the crystal is a d periodic function in the transverse plane and is described by $a_d = a_d(\mathbf{x}/d)$ where $a_d(\mathbf{y})$ is the unit periodic dielectric function taking the values

$$a_d(\mathbf{y}) = \begin{cases} \epsilon_H & \text{in the host material,} \\ \epsilon_P = \epsilon_P(\omega) & \text{in the frequency dependent "plasmonic" material,} \\ \epsilon_R = \epsilon_r/d^2 & \text{in the high dielectric material.} \end{cases} \quad (1.2.4)$$

This choice of high dielectric constant ϵ_R follows that of [9] where ϵ_r has dimensions of area. Setting $h^d(\mathbf{x}) = H_3(\mathbf{x})e^{i(k\hat{\kappa}\cdot\mathbf{x})}$ the Maxwell equations take the form

of the Helmholtz equation given by

$$-\nabla_{\mathbf{x}} \cdot \Big(a_d^{-1}(\frac{\mathbf{x}}{d}) \nabla_{\mathbf{x}} h^d(\mathbf{x}) \Big) = \frac{\omega^2}{c^2} h^d \quad \text{ in } \mathbb{R}^2. \tag{1.2.5}$$

The band structure is given by the Bloch eigenvalues $\frac{\omega^2}{c^2}$ which is a subset of the parameter space $\{\frac{\omega^2}{c^2}, -2\pi \leq k_1 \leq 2\pi, -2\pi \leq k_2 \leq 2\pi\}$, with $k = (k_1^2 + k_2^2)^{1/2}$ and $\hat{\kappa}_i = k_i/k$. This constitutes the first Brillouin Zone for this problem.

We set $\mathbf{x} = d\mathbf{y}$ for $\mathbf{y}$ inside the unit period $Y = [0,1]^2$, put $\beta = dk\hat{\kappa}$ and write $u(\mathbf{y}) = H_3(d\mathbf{y})$. The dependent variable is written $u^d(\mathbf{y}) = h^d(d\mathbf{y}) = u(\mathbf{y}) \exp^{i\beta \cdot \mathbf{y}}$, and we recover the equivalent problem over the unit period cell given by

$$-\nabla_{\mathbf{y}} \cdot \big(a_d^{-1}(\mathbf{y}) \nabla_{\mathbf{y}} u^d \big) = \frac{d^2\omega^2}{c^2} u^d \quad \text{ in } Y. \tag{1.2.6}$$

To proceed we work with the dimensionless ratio $\rho = d/\sqrt{\epsilon_r}$, wave number $\tau = \sqrt{\epsilon_r} k$ and square frequency $\xi = \epsilon_r \frac{\omega^2}{c^2}$. The dimensionless parameter measuring the departure away from the quasi static regime is given by the ratio of period size to wavelength $\eta = dk = \rho\tau \geq 0$. The regime $\eta > 0$ describes dynamic wave propagation while the infinite wavelength or quasi static limit is recovered for $\eta = 0$. Metamaterials by definition are structured materials operating in the sub-wavelength regime $0 < \eta < 1$ away from the quasistatic limit [35]. For these parameters the dielectric permittivity takes the values $\epsilon_P = 1 - \frac{\epsilon_r \omega_p^2/c^2}{\xi}$, $\epsilon_R = \frac{1}{\rho^2}$, $\epsilon_H = 1$, and is denoted by $a_\rho(\mathbf{y})$ for $\mathbf{y}$ in Y and (1.2.6) is given by

$$-\nabla_{\mathbf{y}} \cdot \big(a_\rho^{-1}(\mathbf{y}) \nabla_{\mathbf{y}} u^d(\mathbf{y}) \big) = \rho^2 \xi u^d(\mathbf{y}) \quad \text{ in } Y. \tag{1.2.7}$$

The unit period cell for the generic metamaterial system is represented in Figure 1.1. In what follows R represents the rod cross section containing high dielectric material, P the cross section containing the plasmonic material and H denotes the connected host material region.

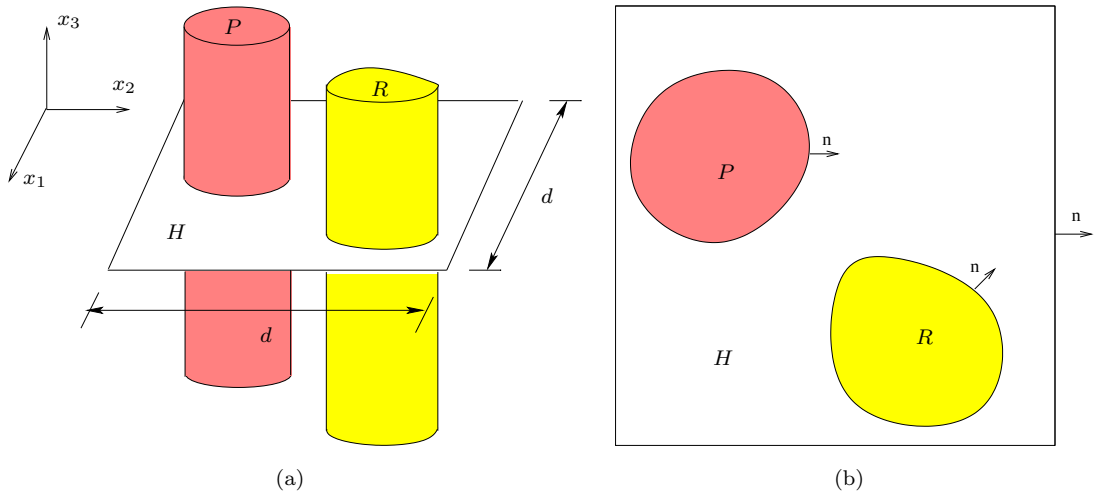

FIGURE 1.1: H represents the host material, P the plasmonic rod and R the high dielectric rod; (a) period cell; (b) cross section of period cell.

In Chapter 2, the generalized electrostatic spectra is introduced and discussed. It is shown to be given by the eigenvalues of a compact operator acting on an appropriate Sobolev space of periodic functions. The electrostatic spectra can be used to characterize the frequency intervals where either double negative or double positive bulk properties appear. The methods are illustrated for ϵ_P given by (1.2.1), however they apply to dielectrics characterized by single oscillator or multiple oscillator models that include dissipation and are of the form

$$\epsilon_P(\omega) = 1 + \sum_{j=1}^{N} \frac{\omega_p^2}{\omega_j^2 - \omega^2 - i\gamma_j\omega}, \tag{1.2.8}$$

where ω_j are resonant frequencies, and γ_j are damping factors.

In Chapter 3, we develop a rigorous method for calculating the frequency intervals where either double negative or double positive bulk properties appear and show how these intervals imply the existence of Bloch wave modes in the dynamic regime away from the quasi static limit. It is shown that the band structure for the metamaterial is characterized by a power series in η and is governed by two distinct types of spectra determined by the shape and configuration of the rods inside the period cells. The series delivers the explicit relationship connecting the

leading order influence of quasi static behavior, as mediated by *effective magnetic permeability and dielectric permittivity*, to the propagation of Bloch wave solutions inside metamaterial crystals made from sub-wavelength $1 > \eta > 0$ structures. The relevant spectra for this problem is found to be given by the Dirichlet spectra for the Laplacian over the rod cross sections R together with a generalized electrostatic spectra associated with the infinite connected region exterior to the rods. These spectra provide two distinct criteria that taken together are sufficient for the existence of power series solutions see, Theorem 3.3.2. The power series is developed in terms of a hierarchy of boundary value problems posed separately over the domain R and the domain exterior to the high dielectric rod $Y \setminus R$. The existence of solutions for the boundary value problems inside the high dielectric rod R is controlled by the Dirichlet spectra. Existence of solutions for boundary value problems exterior to R are determined by the generalized electrostatic spectrum (Chapter 2). We also apply the power series representation to calculate the average Poynting vector and show that in the homogenization limit the energy flow and phase velocity are in opposite directions over frequency intervals associated with double negative behavior. This gives the requisite explicit and mathematically rigorous analysis beyond the homogenization limit and provides evidence for wave propagation in the double negative regime for this class of metamaterial.

The generic class of double negative metamaterials introduced here appears to be new. The motivation behind their construction draws from earlier investigations. The influence of electrostatic resonances on the effective dielectric tensor associated with crystals made from a single frequency dependent dielectric inclusion is developed in the seminal work of [5, 27, 28, 33], see also the more recent work [43] in the context of matematerials. These resonances are responsible for negative effective dielectric permittivity. In this context we point out that the sub-wavelength

geometry introduced here is a three phase medium and the categorization of all possible electrostatic resonances requires a different approach. On the other hand Dirichlet resonances generate negative effective permeability inside high contrast non-dispersive dielectric inclusions, this phenomena is discovered in [9, 10, 15], see also the mathematically related investigations of [12, 22, 25, 53]. Motivated by these observations we have constructed a hybrid composite crystal that combines both high dielectric inclusions and frequency dependent inclusions for generating double negative response from non-magnetic materials.

The power series approach to sub-wavelength $\eta < 1$ analysis has been developed in [20] for characterizing the dynamic dispersion relations for Bloch waves inside plasmonic crystals. It has also been applied to assess the influence of effective negative permeability on the propagation of Bloch waves inside high contrast dielectrics [21], the generation of negative permeability inside metallic - dielectric resonators [42], and for concentric coated cylinder assemblages generating a double negative media [11].

Earlier related work introduces the use of high contrast structures for opening band gaps in photonic crystals [16, 17, 18]. For two phase high contrast media integral equation methods are applied to recover dispersion relations about frequencies corresponding to Dirichlet eigenvalues [3] and [4]. The connection between high contrast interfaces and negative effective magnetic permeability for time harmonic waves is made in [26].

In Chapter 4, we construct metamaterials made from subwavelength periodic arrangements of nonmagnetic infinitely long coated cylinders immersed in a nonmagnetic host. The coated cylinders are parallel to the x_3 axis and made from a frequency independent high dielectric core and a frequency dependent dielectric plasmonic coating (Figure 1.2). We apply the methods to such a metamaterial

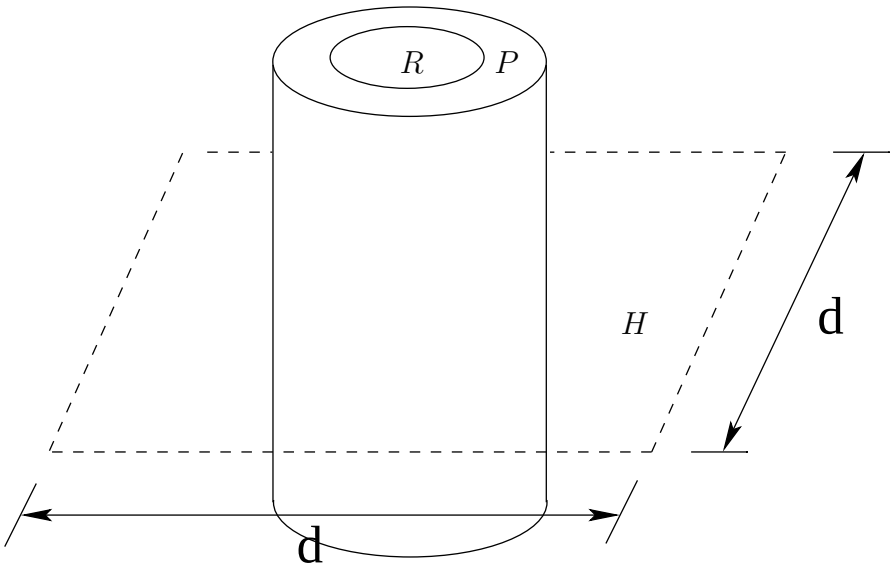

FIGURE 1.2: Coated cylinder microgeometry: R represents the high dielectric core, P the plasmonic coating and H denotes the connected host material.

making use of the method of Rayleigh [45] to numerically calculate the generalized electrostatic resonances. These resonances together with the Dirichlet spectra of the core are used to identify explicit frequency intervals over which effective properties are double negative or double positive. Several branches of the leading order dispersion relation are calculated using the spectral representation formulas for the effective magnetic permeablity and dielelectric constant. We compare these with direct numerical simulations to find that the leading order dispersion relation is a good predictor of the dispersive behavior of the metamaterial. It is found that the leading order behavior trends with the direct numerical simulation even when the length scale of the microstructure is only 20% smaller than the wavelength of the propagating wave. These results provide new methods necessary to identify frequency intervals characterized by negative index behavior and its influence on wave propagation beyond the homogenization limit.

Chapter 2
Foundations

In Chapter 2 and Chapter 3, we consider a metamaterial crystal with period cells containing two parallel infinitely long rods, the frequency dependent plasmonic rod and the frequency independent dielectric rod. The microgeometry of cell is given by Figure 1.1.

2.1 Background

First we outline the steps in the power series development of Bloch waves and establish the mathematical foundations for establishing existence of power series solutions which is discussed in Chapter 3. We introduce the function space $H^1_{per}(Y)$ defined to be all Y-periodic, complex valued square integrable functions with square integrable derivatives with the usual inner product and norm given by

$$(u,v)_Y = \int_Y (\nabla u \cdot \nabla \overline{v} + u\overline{v})\ dy \text{ and } \|u\|_Y = (u,u)_Y^{1/2}. \tag{2.1.1}$$

We also introduce the space $H^1_{per}(Y \setminus R)$ given by all Y-periodic, complex valued square integrable functions with square integrable derivatives and the inner product and seminorm

$$(u,v) = \int_{Y\setminus R} \nabla u \cdot \nabla \overline{v}\, dy \text{ and } \|u\| = (u,u)^{1/2}. \tag{2.1.2}$$

The variational form of (1.2.7) is given by

$$\int_Y a_\rho^{-1} \nabla u^d \cdot \nabla \bar{\tilde{v}} = \int_Y \frac{\rho^2 \xi}{c^2} u^d \bar{\tilde{v}} \tag{2.1.3}$$

for any $\tilde{v} = v(\mathbf{y})e^{i\hat{\kappa}\cdot\tau\rho\mathbf{y}}$, where $v \in H^1_{per}(Y)$. On writing $u^d = u(\mathbf{y})e^{i\hat{\kappa}\cdot\tau\rho\mathbf{y}}$ and setting $\eta = \tau\rho$ we transform (2.1.3) into

$$\int_H \tau^2(\xi - \epsilon_r\frac{\omega_p^2}{c^2})(\nabla + i\eta\hat{\kappa})u \cdot \overline{(\nabla + i\eta\hat{\kappa})v} + \int_P \tau^2\xi(\nabla + i\eta\hat{\kappa})u \cdot \overline{(\nabla + i\eta\hat{\kappa})v}$$
$$+ \int_R \eta^2(\xi - \epsilon_r\frac{\omega_p^2}{c^2})(\nabla + i\eta\hat{\kappa})u \cdot \overline{(\nabla + i\eta\hat{\kappa})v} = \int_Y \eta^2\xi(\xi - \epsilon_r\frac{\omega_p^2}{c^2})u\overline{v} \qquad (2.1.4)$$

We introduce the power series

$$u = \sum_{m=0}^{\infty} \eta^m u_m \qquad (2.1.5)$$

$$\xi = \sum_{m=0}^{\infty} \eta^m \xi_m \qquad (2.1.6)$$

where u_m belongs to $H^1_{per}(Y)$. In view of the algebra it is convenient to write $u_m = i^m \underline{u}_0 \psi_m$ where $\underline{u}_0$ is an arbitrary constant factor.

We now describe the underlying variational structure associated with the power series solution. Set

$$z = \epsilon_P^{-1}(\xi_0) = \left(1 - \frac{\epsilon_r\omega_p^2/c^2}{\xi_0}\right)^{-1}$$

and for u, v belonging to $H^1_{per}(Y)$ we introduce the sesquilinear form

$$B_z(u, v) = \int_H \nabla u \cdot \nabla\overline{v}\, d\mathbf{y} + \int_P z\, \nabla u \cdot \nabla\overline{v}\, d\mathbf{y}. \qquad (2.1.7)$$

Here the form $B_z(u, v)$ is well defined for functions in $H^1_{per}(Y\backslash R)$ and $Y\backslash R = H\cup P$. Substitution of the series into the system (2.1.4) and equating like powers of η,

produces the infinite set of coupled equations for $m = 0, 1, 2 \ldots$ given by

$$
\begin{aligned}
&\tau^2 B_z(\psi_m, v) \\
&+\xi_0^{-1}\epsilon_p^{-1}(\xi_0)\tau^2 \int_{Y\setminus R} \Big[\sum_{l=1}^{m-1} (-i)^l \xi_l \nabla\psi_{m-l} \cdot \nabla\overline{v} \\
&+\hat{\kappa} \cdot \sum_{l=0}^{m-1} (-i)^l \xi_l (\psi_{m-1-l}\nabla\overline{v} - \nabla\psi_{m-1-l}\overline{v}) - \sum_{l=0}^{m-2} (-i)^l \xi_l \psi_{m-2-l}\overline{v}\Big] \\
&-\xi_0^{-1}\epsilon_p^{-1}(\xi_0)\tau^2\epsilon_r \frac{\omega_p^2}{c^2} \int_H \big[\hat{\kappa} \cdot (\psi_{m-1}\nabla\overline{v} - \nabla\psi_{m-1}\overline{v}) - \psi_{m-2}\overline{v}\big] \\
&-\xi_0^{-1}\epsilon_p^{-1}(\xi_0) \int_R \Big[\sum_{l=0}^{m-2} (-i)^l \xi_l \nabla\psi_{m-2-l} \cdot \nabla\overline{v} \\
&+\hat{\kappa} \sum_{l=0}^{m-3} (-i)^l \xi_l (\psi_{m-3-l}\nabla\overline{v} - \nabla\psi_{m-3-l}\overline{v}) - \sum_{l=0}^{m-4} (-i)^l \xi_l \psi_{m-4-l}\overline{v}\Big] \\
&+\xi_0^{-1}\epsilon_p^{-1}(\xi_0) \int_R \epsilon_r \frac{\omega_p^2}{c^2} \big[\nabla\psi_{m-2} \cdot \nabla\overline{v} + \hat{\kappa}(\psi_{m-3}\nabla\overline{v} - \nabla\psi_{m-3}\overline{v}) + \psi_{m-4}\overline{v}\big] \\
&-\xi_0^{-1}\epsilon_p^{-1}(\xi_0) \int_Y \Big[\sum_{l=0}^{m-2} \sum_{n=0}^{l} \xi_{m-2-l}\xi_n \psi_{l-n} i^{l-n-m}\overline{v} + \epsilon_r \frac{\omega_p^2}{c^2} \sum_{l=0}^{m-2} (-i)^l \xi_l \psi_{m-2-l}\overline{v}\Big] \\
&= 0, \text{ for all } v \text{ in } H^1_{per}(Y).
\end{aligned}
\tag{2.1.8}
$$

Here the convention is $\psi_m = 0$ for $m < 0$.

The determination of $\{\psi_m\}_{m=0}^{\infty}$ proceeds iteratively. We start by determining ψ_0 on $Y \setminus R$, this function is used as boundary data to determine ψ_0 in R from which we determine ψ_1 on $Y \setminus R$ and the full sequence is determined on iterating this cycle. The elements ξ_m are recovered from solvability conditions obtained by setting $v = 1$ in (2.1.8) and proceeding iteratively. The complete algorithm together with explicit boundary value problems necessary for the determination of the sequences $\{\psi_m\}_{m=0}^{\infty}$, $\{\xi_m\}_{m=0}^{\infty}$ is described in Chapter 3.2.

The existence theory for the solution of the sequence of boundary value problems is based on the sesquilinear form $B_z(u, v)$ defined for functions u and v belonging to $H^1_{per}(Y \setminus R)/\mathbb{C}$. Here $H^1_{per}(Y \setminus R)/\mathbb{C}$ is the subspace of functions u belonging to $H^1_{per}(Y \setminus R)$ with zero mean $\int_{Y\setminus R} u\, dy = 0$. This space is a Hilbert space with

inner product (2.1.2). Although in this treatment ϵ_P is given by (1.2.1) we are motivated by the general case (1.2.8) and proceed in full generality allowing for the possibility that z can lie anywhere on the complex plane $\mathbb{C}$ including the negative real axis. Thus for each z in $\mathbb{C}$ we are required to characterize the range of the map $u \mapsto B_z(u, \cdot)$ viewed as a linear transformation T_z mapping u into the space of bounded skew linear functionals on $H^1_{per}(Y \setminus R)/\mathbb{C}$. This is linked to the following eigenvalue problem characterizing all pairs λ in $\mathbb{C}$, ψ in $H^1_{per}(Y \setminus R)/\mathbb{C}$ that solve

$$-\frac{1}{2}\int_P \nabla\psi \cdot \nabla\overline{v}\, d\mathbf{y} + \frac{1}{2}\int_H \nabla\psi \cdot \nabla\overline{v}\, d\mathbf{y} = (\lambda\psi, v), \tag{2.1.9}$$

for every v in $H^1_{per}(Y \setminus R)/\mathbb{C}$. Inspection shows that for $z = (\lambda + 1/2)/(\lambda - 1/2)$ that $B_z(\psi, v) = 0$, for every v in $H^1_{per}(Y \setminus R)/\mathbb{C}$. In other words the kernel of the operator T_z is nonempty for $z = (\lambda + 1/2)/(\lambda - 1/2)$. The eigenvalues λ will be referred to as generalized electrostatic resonances. In what follows we show that T_z is a one to one and onto map from $H^1_{per}(Y \setminus R)/\mathbb{C}$ into the dual space provided that $z \neq (\lambda + 1/2)/(\lambda - 1/2)$.

2.2 Two basic theorems

The generalized electrostatic resonances are characterized by introducing a suitable orthogonal decomposition of $H^1_{per}(Y \setminus R)/\mathbb{C}$. We introduce the subspace $H^1_0(P)$ given by the closure in the H^1 norm of smooth functions v with compact support on P and the subspace $H^1_{0,per}(H)$ given by the closure in the H^1 norm of all periodic continuously differentiable functions with support outside P. Extending elements of $H^1_{0,per}(H)$ by zero to $Y \setminus R$ delivers $W_1 \subset H^1_{per}(Y \setminus R)$, extending elements of $H^1_0(P)$ by zero to $Y \setminus R$ delivers $W_2 \subset H^1_{per}(Y \setminus R)$. Define W_3 to be all functions w in $H^1_{per}(Y \setminus R)$ for which the boundary integral $\int_{\partial P} w\, dS$ vanishes and that belong to the orthogonal complement of $W_1 \cup W_2$ with respect to the inner product (2.1.2).

Its easily verified that W_1, W_2, and W_3 are pairwise orthogonal with respect to the inner product (2.1.2) and

$$H^1_{per}(Y \setminus R)/\mathbb{C} = W_1 \oplus W_2 \oplus W_3 \oplus \mathbb{C}, \tag{2.2.1}$$

where the constant part of a function u belonging to this space is uniquely determined by the condition $\int_{Y\setminus R} u\, dy = 0$.

The following theorem describing all eigenvalue eigenfunction pairs is established in Chapter 2.3.

Theorem 2.2.1. *The eigenvalues for* (2.1.9) *are real and constitute a denumerable set contained inside* $[-1/2, 1/2]$ *with the only accumulation point being zero. The eigenspaces associated with* $\lambda = 1/2$ *and* $\lambda = -1/2$ *are* W_1 *and* W_2 *respectively. Eigenspaces associated with distinct eigenvalues in* $(-1/2, 1/2)$ *are finite dimensional, pairwise orthogonal, and their union spans the subspace* W_3.

We denote the denumerable set of eigenvalues for (2.1.9) by the sequence $\{\lambda_i\}_{i=1}^{\infty}$. The orthogonal projections onto W_1 and W_2 are denoted by $\mathcal{P}_1$ and $\mathcal{P}_2$. The orthogonal projections on to the finite dimensional eigenspaces associated with the eigenvalues λ_i in $(-1/2, 1/2)$ are denoted by $\mathcal{P}_{\lambda_i}$. For $z \neq (\lambda_i + 1/2)/(\lambda_i - 1/2)$ the following existence theorem holds.

Theorem 2.2.2. *Suppose* $z \neq (\lambda_i + 1/2)/(\lambda_i - 1/2)$ *for* $\lambda_i \in [-\frac{1}{2}, \frac{1}{2}]$ *then*

- *For any* $F \in \left[H^1_{per}(Y \setminus R)/\mathbb{C}\right]^*$ *such that* $F(v) = 0$ *for constant* v*, there exists a unique solution* $u \in H^1_{per}(Y \setminus R)/\mathbb{C}$ *of the variational problem* $B_z(u, v) = \overline{F(v)}$ *for all* $v \in H^1_{per}(Y \setminus R)/\mathbb{C}$.

- *The transformation T_z from $H^1_{per}(Y \setminus R)/\mathbb{C}$ onto itself has the representation formula given by*

$$T_z = \mathcal{P}_1 + z\mathcal{P}_2 + \sum_{-\frac{1}{2}<\lambda_n<\frac{1}{2}} (1 + (z-1)(\frac{1}{2} - \lambda_n))\mathcal{P}_{\lambda_n}, \tag{2.2.2}$$

with inverse

$$T_z^{-1} = \mathcal{P}_1 + z^{-1}\mathcal{P}_2 + \sum_{-\frac{1}{2}<\lambda_n<\frac{1}{2}} (1 + (z-1)(\frac{1}{2} - \lambda_n))^{-1}\mathcal{P}_{\lambda_n}, \tag{2.2.3}$$

and $B_z(u,v) = (T_z u, v)$ for all u, v in $H^1_{per}(Y \setminus R)/\mathbb{C}$.

This theorem is proved in Chapter 2.4.

2.3 Generalized electrostatic spectra

In this part we establish Theorem 2.2.1 and characterize all pairs (λ, ψ) in $\mathbb{C} \times H^1_{per}(Y \setminus R)$ satisfying (2.1.9). We start by recalling the bilinear form in (2.1.9) and forming the quotient

$$Q(u) = \frac{-\frac{1}{2}\int_P |\nabla u|^2\, dx + \frac{1}{2}\int_H |\nabla u|^2\, dx}{(u,u)}. \tag{2.3.1}$$

From (2.3.1) it is evident that λ lies inside $[-1/2, 1/2]$. It is easily seen that the solutions (λ, ψ) of (2.1.9) for the choices $\lambda = \frac{1}{2}$ and $\lambda = -\frac{1}{2}$ correspond to ψ in W_1 and W_2 respectively. Only the 0 element of W_3 satisfies (2.1.9) for the choices $\lambda = \frac{1}{2}$ and $\lambda = -\frac{1}{2}$.

We now investigate solutions (λ, ψ) for ψ belonging to W_3. The bilinear form (2.1.9) defines a map T from W_3 into the space of skew linear functionals on W_3. Here W_3 is a Hilbert space and

$$(Tu, v) = -\frac{1}{2}\int_P \nabla u \cdot \nabla \overline{v}\, d\mathbf{y} + \frac{1}{2}\int_H \nabla u \cdot \nabla \overline{v}\, d\mathbf{y}, \tag{2.3.2}$$

for u and v in W_3. In what follows we show that T is a compact map from W_3 onto W_3 with eigenvalues contained inside the open interval $(-1/2, 1/2)$. We do this by

providing an explicit representation for T given in terms of a composition of single and double layer potentials.

Set $\mathbb{D} = \cup_{n\in\mathbb{Z}^2}((Y \setminus R) + n)$ and introduce the Green's function $G(\mathbf{x}, \mathbf{y})$ on $\mathbb{D}$ such that: G is separately periodic in $\mathbf{x}$ and $\mathbf{y}$ with period Y, G is C^2 in each of the variables $\mathbf{x}$ and $\mathbf{y}$ for $\mathbf{x} \neq \mathbf{y}$, and

$$\begin{aligned} &\Delta_{\mathbf{x}} G(\mathbf{x}, \mathbf{y}) = \sum_{n\in\mathbb{Z}^2} \delta(\mathbf{x} - \mathbf{y} + n) - 1 \text{ in } \mathbb{D}, \\ &\partial_{n_{\mathbf{x}}} G(\mathbf{x}, \mathbf{y}) = \frac{|R|}{|\partial R|}, \text{ for } \mathbf{x} \in \cup_{n\in\mathbb{Z}^2}(\partial R + n), \end{aligned} \tag{2.3.3}$$

where $\delta_{\mathbf{x}}$ is the Dirac delta function located at $\mathbf{x}$ and $|R|$ and $|\partial R|$ are the area and arc-length of R and ∂R respectively. We can find $G(\mathbf{x}, \mathbf{y})$ as a sum of the periodic free space Green's function F for the Laplacian and a corrector ϕ^*: $G(\mathbf{x}, \mathbf{y}) = F(\mathbf{x}, \mathbf{y}) + \phi^*(\mathbf{x}, \mathbf{y})$, where

$$F(x, y) = -\sum_{n\in\mathbb{Z}^2\setminus\{0\}} \frac{e^{i2\pi n\cdot(x-y)}}{4\pi^2|n|^2}, \tag{2.3.4}$$

$\phi^*(\mathbf{x}, \mathbf{y})$ is periodic in $\mathbf{x}$ and $\mathbf{y}$ with period Y, C^2 in $\mathbf{x}$, $\mathbf{y}$, and solves

$$\begin{aligned} &\Delta_{\mathbf{x}}\phi^*(\mathbf{x}, \mathbf{y}) = 0 \text{ for } \mathbf{x}, \mathbf{y} \text{ in } \mathbb{D}, \\ &\partial_{n_{\mathbf{x}}}\phi^*(\mathbf{x}, \mathbf{y})_{|^+_{\partial R}} = -\partial_{n_{\mathbf{x}}} F(\mathbf{x}, \mathbf{y})_{|^+_{\partial R}} + \frac{|R|}{|\partial R|}, \text{for } \mathbf{x} \text{ on } \partial R, \\ &\text{and } \int_{\partial R} \phi^*(\mathbf{x}, \mathbf{y}) dS_{\mathbf{x}} = 0. \end{aligned} \tag{2.3.5}$$

Here the subscript ∂R^+, indicates traces of functions on ∂R taken from the outside of R.

Lemma 2.3.1.

$$\begin{aligned} G(\boldsymbol{y}, \boldsymbol{x}) = \quad & G(\boldsymbol{x}, \boldsymbol{y}) + \int_{Y\setminus R} (G(\boldsymbol{z}, \boldsymbol{x}) - G(\boldsymbol{z}, \boldsymbol{y}))\, d\boldsymbol{z} \\ & + \frac{|R|}{|\partial R|} \int_{\partial R} (G(\boldsymbol{z}, \boldsymbol{y}) - G(\boldsymbol{z}, \boldsymbol{x}))\, dS_{\boldsymbol{z}}. \end{aligned} \tag{2.3.6}$$

Proof. From (2.3.3), it is easy to get

$$\int_{Y\setminus R} G(\mathbf{z},\mathbf{x})\Delta_{\mathbf{z}} G(\mathbf{z},\mathbf{y})\,d\mathbf{z} = G(\mathbf{y},\mathbf{x}) - \int_{Y\setminus R} G(\mathbf{z},\mathbf{x})\,d\mathbf{z} \tag{2.3.7}$$

and

$$\int_{Y\setminus R} G(\mathbf{z},\mathbf{y})\Delta_{\mathbf{z}} G(\mathbf{z},\mathbf{x})\,d\mathbf{z} = G(\mathbf{x},\mathbf{y}) - \int_{Y\setminus R} G(\mathbf{z},\mathbf{y})\,d\mathbf{z}. \tag{2.3.8}$$

On the other hand, we have

$$\begin{aligned}
&\int_{Y\setminus R} G(\mathbf{z},\mathbf{x})\Delta_{\mathbf{z}} G(\mathbf{z},\mathbf{y})\,d\mathbf{z} \\
&= \int_{Y\setminus R} \nabla_{\mathbf{z}}\cdot\left(G(\mathbf{z},\mathbf{x})\nabla_{\mathbf{z}} G(\mathbf{z},\mathbf{y})\right)d\mathbf{z} - \int_{Y\setminus R} \nabla_{\mathbf{z}} G(\mathbf{z},\mathbf{x})\cdot\nabla_{\mathbf{z}} G(\mathbf{z},\mathbf{y})\,d\mathbf{z} \\
&= -\frac{|R|}{|\partial R|}\int_{\partial R} G(\mathbf{z},\mathbf{x})\,dS_{\mathbf{z}} - \int_{Y\setminus R} \nabla_{\mathbf{z}} G(\mathbf{z},\mathbf{x})\cdot\nabla_{\mathbf{z}} G(\mathbf{z},\mathbf{y})\,d\mathbf{z}.
\end{aligned} \tag{2.3.9}$$

Hence (2.3.7) and (2.3.9) give

$$\begin{aligned}
&G(\mathbf{y},\mathbf{x}) - \int_{Y\setminus R} G(\mathbf{z},\mathbf{x})\,d\mathbf{z} + \frac{|R|}{|\partial R|}\int_{\partial R} G(\mathbf{z},\mathbf{x})\,dS_{\mathbf{z}} \\
&= -\int_{Y\setminus R} \nabla_{\mathbf{z}} G(\mathbf{z},\mathbf{x})\cdot\nabla_{\mathbf{z}} G(\mathbf{z},\mathbf{y})\,d\mathbf{z}.
\end{aligned} \tag{2.3.10}$$

Similarly, we have

$$\begin{aligned}
&G(\mathbf{x},\mathbf{y}) - \int_{Y\setminus R} G(\mathbf{z},\mathbf{y})\,d\mathbf{z} + \frac{|R|}{|\partial R|}\int_{\partial R} G(\mathbf{z},\mathbf{y})\,dS_{\mathbf{z}} \\
&= -\int_{Y\setminus R} \nabla_{\mathbf{z}} G(\mathbf{z},\mathbf{y})\cdot\nabla_{\mathbf{z}} G(\mathbf{z},\mathbf{x})\,d\mathbf{z}.
\end{aligned} \tag{2.3.11}$$

(2.3.10) and (2.3.11) finish the proof. □

The space of mean zero square integrable functions defined on ∂P is denoted by $L_0^2(\partial P)$ and for ϕ in $L_0^2(\partial P)$ the single layer potential $\tilde{S}_P$ is given by

$$\tilde{S}_P(\phi) = \int_{\partial P} G(\mathbf{x},\mathbf{y})\phi(\mathbf{y})dS_{\mathbf{y}}. \tag{2.3.12}$$

Lemma 2.3.2. *For $\phi \in L_0^2(\partial P)$,*

$$\int_{Y\setminus R} \nabla u \cdot \nabla(\tilde{S}_P\phi) = -\int_{\partial P} \phi u \, dS_{\boldsymbol{x}} \quad \forall u \in W_3. \tag{2.3.13}$$

Proof. This can be proved by the facts that the normal derivative of $\tilde{S}_P\phi$ on ∂R equals 0; and

$$\partial_n \tilde{S}_P\phi(\mathbf{x})|_{\partial P\pm} = \pm\frac{1}{2}\phi + K^*\phi. \tag{2.3.14}$$

Here n is the outward unit normal to P and the $+$ and the $-$ refer to the traces from the interior and exterior of P. $K^*\phi(\mathbf{x}) = P.V. \int_{\partial P} \partial_{n_{\mathbf{x}}} G(\mathbf{x},\mathbf{y})\phi(y)\, dS_{\mathbf{y}}$, where $P.V.$ denotes the principle value. □

Lemma 2.3.3. *The kernel of the single layer potential $\tilde{S}_P$ is 0.*

Proof. Let ϕ belong to the kernel of $\tilde{S}_P$. Then $\tilde{S}_P\phi|_{\partial P} = 0$. Since $\tilde{S}_P\phi \in H^1_{per}(Y\setminus R)$ and $\Delta_{\mathbf{x}}\tilde{S}_P\phi = 0$ in H and P, we see that $\tilde{S}_P\phi = 0$ in $Y \setminus R$. From Lemma 2.3.2, $\phi|_{\partial P}$ is a constant. Because $\phi \in L_0^2(\partial P)$, $\phi = 0$. □

Now we define $\tilde{S}_P^*$ be the adjoint operator of $\tilde{S}_P$ such that for $\phi \in L_0^2(\partial P)$, $\tilde{S}_P^*\phi(\mathbf{x}) = \int_{\partial P} G(\mathbf{y},\mathbf{x})\phi(\mathbf{y})\, d\mathbf{y}$. From Lemma 2.3.1,

$$\begin{aligned} \tilde{S}_P^*\phi(\mathbf{x}) = \quad & \tilde{S}_P\phi(\mathbf{x}) - \int_{Y\setminus R} \tilde{S}_P\phi(\mathbf{z})\, d\mathbf{z} \\ & + \frac{|R|}{|\partial R|}\int_{\partial R} \tilde{S}_P\phi(\mathbf{z})\, dS_{\mathbf{z}} \quad \text{for } \phi \in L_0^2(\partial P). \end{aligned} \tag{2.3.15}$$

With the help of (2.3.15) it is not hard to prove that the kernel of $\tilde{S}_P^*$ is also 0.

We introduce the modified single layer potential S_P mapping $L_0^2(\partial P)$ into W_3 given by

$$S_P(\phi) = \tilde{S}_P(\phi) - |\partial P|^{-1}\int_{\partial P} \tilde{S}_P(\phi)(\mathbf{y}) dS_{\mathbf{y}}. \tag{2.3.16}$$

On restricting $S_P(\phi)(\mathbf{x})$ to $\mathbf{x}$ on ∂P, S_P is a bounded map from $L_0^2(\partial P)$ onto $H^{1/2}(\partial P) \cap L_0^2(\partial P)$. The following theorem tells us that this map is also self-adjoint, one-to-one and onto.

Theorem 2.3.4. *Suppose we restrict $S_P(\phi)(\boldsymbol{x})$ to $\boldsymbol{x}$ on ∂P. S_P is self-adjoint with respect to the $L^2(\partial P)$ inner product and is a bounded one to one linear map from $L_0^2(\partial P)$ onto $H^{1/2}(\partial P) \cap L_0^2(\partial P)$.*

Proof. Suppose ψ and $\phi \in L_0^2(\partial P)$. By the definition (2.3.16),

$$\int_{\partial P} \tilde{S}_P \phi \psi = \int_{\partial P} S_P \phi \psi. \tag{2.3.17}$$

On the other hand, using (2.3.15), we have

$$\int_{\partial P} \tilde{S}_P \phi \psi = \int_{\partial P} \phi \tilde{S}_P^* \psi = \int_{\partial P} \phi S_P \psi \tag{2.3.18}$$

The above two equations show that S_P is self-adjoint.

Next we will show the kernel of S_P is 0. Suppose $\hat{\phi}$ belongs to the kernel of S_P. Then $S_P(\hat{\phi}) = \tilde{S}_P(\hat{\phi}) - |\partial P|^{-1} \int_{\partial P} \tilde{S}_P(\hat{\phi})\, dS$. For any u in W_3, we have

$$\int_{Y \setminus R} \nabla u \cdot \nabla S_P \hat{\phi} = \int_{\partial P} [\partial_n u]_+^- S_P \hat{\phi} = 0 \tag{2.3.19}$$

While through Lemma 2.3.2 and the definition of S_P, we get

$$\int_{Y \setminus R} \nabla u \cdot \nabla S_P \hat{\phi} = \int_{Y \setminus R} \nabla u \cdot \nabla \tilde{S}_P \hat{\phi} = -\int_{\partial P} \hat{\phi} u \, dS. \tag{2.3.20}$$

Therefore the fact $\hat{\phi} \in L_0^2(\partial P)$ shows that $\hat{\phi} = 0$. Hence S_P is one-to-one. Last we show this map is onto. Denote the closure of $R(S_P)$ with respect to $H^{\frac{1}{2}}$ by $\overline{R(S_P)}$ where $R(S_P)$ is the range of S_P. Then we have

$$R(S_P)^\perp = Ker(S_P) = \{0\} = \overline{R(S_P)}^\perp. \tag{2.3.21}$$

Suppose $R(S_P)$ is a subspace of $H^{1/2}(\partial P) \cap L_0^2(\partial P)$. Therefore there exists a complementary subspace V such that $H^{1/2}(\partial P) \cap L_0^2(\partial P) = R(S_P) \oplus V$. However

$$H^{1/2}(\partial P) \cap L_0^2(\partial P) = \overline{R(S_P)} \oplus \overline{R(S_P)}^\perp = \overline{R(S_P)} \tag{2.3.22}$$

If $V \neq \{0\}$, then

$$H^{1/2}(\partial P) \cap L_0^2(\partial P) = \overline{span\{R(S_P) \cup V\}}$$
$$\supset \overline{R(S_P)} = H^{1/2}(\partial P) \cap L_0^2(\partial P). \tag{2.3.23}$$

Hence $H^{1/2}(\partial P) \cap L_0^2(\partial P) = R(S_P)$, i.e., the map S_P is onto. □

Hence the inverse denoted by $S_{\partial P}^{-1} : H^{1/2}(\partial P) \cap L_0^2(\partial P) \to L_0^2(\partial P)$ is linear and continuous. We introduce the trace operator γ mapping W_3 into $H^{1/2}(\partial P) \cap L_0^2(\partial P)$, this map is bounded and onto [2]. Collecting results we have the following

Lemma 2.3.5. *S_p is a one to one, bounded linear transformation from $L_0^2(\partial P)$ onto W_3 with $S_P^{-1} : W_3 \to L_0^2(\partial P)$ linear and continuous given by $S_P^{-1} = S_{\partial P}^{-1}\gamma$.*

Proof. Given u in W_3 consider its trace on ∂P given by $\gamma u = u_{|\partial P}$ and $u_{|\partial P}$ belongs to $H^{1/2}(\partial P) \cap L_0^2(\partial P)$. For $\mathbf{x}$ in $Y \setminus R$ set $w(\mathbf{x}) = S_P(S_{\partial P}^{-1}(u_{|\partial P}))(\mathbf{x})$. Since w belongs to W_3 the difference $w - u$ also belongs to W_3. Noting further that the traces of w and u agree on ∂P we conclude that $w - u$ also belongs to $W_1 \oplus W_2$. However since $W_3 = (W_1 \oplus W_2)^{\perp}$ it is evident that $w - u = 0$ and we conclude that $S_P^{-1} = S_{\partial P}^{-1}\gamma$. □

The outward pointing normal derivative of a quantity q on ∂P is denoted by $\frac{\partial q}{\partial n_{\mathbf{x}}}$ and the jump relations satisfied by the single layer potential are given by

$$S_P(\phi)_{|_{\partial P}^{+}} = S_P(\phi)_{|_{\partial P}^{-}}, \text{ on } \partial P, \frac{\partial S_P(\phi)}{\partial n_{\mathbf{x}}}|_{\partial P_{-}^{+}} = \pm\frac{1}{2}\phi + K_P^*(\phi), \text{ on } \partial P \tag{2.3.24}$$

where the double layer K_P^* is a bounded linear operator mapping $L_0^2(\partial P)$ into $L_0^2(\partial P)$ defined by

$$K_P^*(\phi) = \int_{\partial P} \frac{\partial G(\mathbf{x}, \mathbf{y})}{\partial n_{\mathbf{x}}} \phi(\mathbf{y}) dS_{\mathbf{y}}, \tag{2.3.25}$$

and the subscripts $+$ and $-$ indicate traces from the outside and inside of P respectively. Here $\frac{\partial G}{\partial n_{\mathbf{x}}}$ is a continuous kernel of order zero and it follows [19] that

K_P^* is a compact operator mapping $L_0^2(\partial P)$ into $L_0^2(\partial P)$. Now we identify the transform T defined by (2.3.2).

Theorem 2.3.6. *The linear map $T : W_3 \to W_3$ defined by the sesquilinear form* (2.3.2) *is given by*

$$T = S_P K_P^* S_P^{-1}, \tag{2.3.26}$$

and is a compact bounded self-adjoint operator on W_3 with eigenvalues lying inside $(-1/2, 1/2)$.

Since T is self-adjoint, bounded, and compact: the spectrum is discrete with only zero as an accumulation point, the eigenspaces associated with distinct eignevalues are pairwise orthogonal, finite dimensional, and their union is W_3. Theorem 2.2.1 follows immediately from Theorem 2.3.6 noting that the choices $\lambda = 1/2$, $\lambda = -1/2$ in (2.1.9) correspond to ϕ belonging to W_1 and W_2 respectively.

We now prove Theorem 2.3.6.

Proof. Step I.

We establish (2.3.26). For u, v, consider

$$(S_P K_p^* S_P^{-1}(u), v) = \int_{Y \setminus R} \nabla S_P K_p^* S_P^{-1}(u) \cdot \nabla \overline{v}\, dx. \tag{2.3.27}$$

Integration by parts gives

$$(S_P K_p^* S_P^{-1}(u), v) = \int_{\partial P} \left[\frac{\partial (S_P K_p^* S_P^{-1}(u))}{\partial n_{\mathbf{x}}} \right]_+^- \overline{v}\, dS, \tag{2.3.28}$$

where $[q]_+^- = q|_{\partial P^-} - q|_{\partial P^+}$. Applying the jump condition (2.3.24) we get

$$(S_P K_p^* S_P^{-1}(u), v) = -\int_{\partial P} K_p^* S_P^{-1}(u) \overline{v}\, dS, \tag{2.3.29}$$

applying (2.3.24) again gives

$$\begin{aligned} K_p^* S_P^{-1}(u) &= \frac{1}{2} \frac{\partial S_P S_P^{-1}(u)}{\partial n_{\mathbf{x}}}|_{\partial P^-} + \frac{1}{2} \frac{\partial S_P S_P^{-1}(u)}{\partial n_{\mathbf{x}}}|_{\partial P^+} \\ &= \frac{1}{2} \frac{\partial u}{\partial n_{\mathbf{x}}}|_{\partial P^-} + \frac{1}{2} \frac{\partial u}{\partial n_{\mathbf{x}}}|_{\partial P^+}. \end{aligned} \tag{2.3.30}$$

Step I now follows on substitution of (2.3.30) into (2.3.29) and integration by parts. Step II. The remaining properties of the operator T follow directly from the representation $T = S_P K_P^* S_P^{-1}$ and the properties of S_P and K_P^*. □

We conclude noting that the spectrum of T is the same as the spectrum of K_P^*. This is stated in the following Lemma.

Lemma 2.3.7. *$Tu = \lambda u$ if and only if λ corresponds to an eigenvalue of K_P^*.*

Proof. If a pair (λ, u) belonging to $(-1/2, 1/2) \times W_3$ satisfies $Tu = \lambda u$ then $S_P K_P^* S_P^{-1} u = \lambda u$. Multiplication of both sides by S_P^{-1} shows that $S_P^{-1} u$ is an eigenfunction for K_P^* associated with λ. Suppose the pair (λ, w) belongs to $(-1/2, 1/2) \times L_0^2(\partial P)$ and satisfies $K_P^* w = \lambda w$. Since the trace map from W_3 to $H^{1/2}(\partial P) \cap L_0^2(\partial P)$ is onto then there is a u in W_3 for which $w = S_P^{-1} u$ and $K_P^* S_P^{-1} u = \lambda S_P^{-1} u$. Multiplication of this identity by S_P shows that u is an eigenfunction for T associated with λ. □

2.4 Existence for exterior problems with a dielectric permitivity in $\mathbb{C}$

In this part we establish Theorem 2.2.2. Recall that any element u of $H^1_{per}(Y \setminus R)/\mathbb{C}$ can be written as

$$u = \mathcal{P}_1 u + \mathcal{P}_2 u + \sum_{-\frac{1}{2} < \lambda_n < \frac{1}{2}} \mathcal{P}_{\lambda_n} u + d. \tag{2.4.1}$$

where d is chosen such that $\int_{Y \setminus R} u \, dy = 0$. Here $\mathcal{P}_i$ are the orthgonal projections onto W_i, $i = 1, 2$ and $\mathcal{P}_{\lambda_n}$ are the orthogonal projections onto the finite dimensional eigenspaces associated with the eigenvalues λ_n in $(-1/2, 1/2)$. The orthogonal decomposition (2.4.1) is used in the proof of Theorem 2.2.2 given below.

Proof. For u, v in $H^1_{per}(Y \setminus R)/\mathbb{C}$ we apply (2.4.1) to see that

$$\begin{aligned} B_z(u,v) &= \sum_{i=1}^{2} B_z(\mathcal{P}_i u, \mathcal{P}_i v) + \sum_{-\frac{1}{2}<\lambda_n<\frac{1}{2}} B_z(\mathcal{P}_{\lambda_n} u, \mathcal{P}_{\lambda_n} v) \\ &= (\mathcal{P}_1 u, v) + z(\mathcal{P}_2 u, v) + \sum_{-\frac{1}{2}<\lambda_n<\frac{1}{2}} (1 + (z-1)(\frac{1}{2} - \lambda_n))(\mathcal{P}_{\lambda_n} u, v) \\ &= (T_z u, v). \end{aligned} \tag{2.4.2}$$

From (2.4.2) we conclude that

$$T_z = \mathcal{P}_1 + z\mathcal{P}_2 + \sum_{-\frac{1}{2}<\lambda_n<\frac{1}{2}} (1 + (z-1)(\frac{1}{2} - \lambda_n))\mathcal{P}_{\lambda_n}. \tag{2.4.3}$$

It is evident from (2.4.3) that for $z \neq (\lambda_n + 1/2)/(\lambda_n - 1/2)$ that T_z is a bounded one to one and onto map in $H^1_{per}(Y \setminus R)/\mathbb{C}$. The formula for T_z^{-1} is given by

$$T_z^{-1} = \mathcal{P}_1 + z^{-1}\mathcal{P}_2 + \sum_{-\frac{1}{2}<\lambda_n<\frac{1}{2}} (1 + (z-1)(\frac{1}{2} - \lambda_n))^{-1}\mathcal{P}_{\lambda_n}. \tag{2.4.4}$$

Taking conjugates on both sides of (2.4.2) gives $\overline{B_z(u,v)} = (v, T_z u)$ and choosing $u = T_z^{-1} q$ for q in $H^1_{per}(Y \setminus R)/\mathbb{C}$ delivers the identity

$$\overline{B_z(T_z^{-1} q, v)} = (v, q). \tag{2.4.5}$$

To complete the proof consider any linear functional F in $[H^1_{per}(Y \setminus R)/\mathbb{C}]^*$ with $F(v) = 0$ for $v = const.$ Applying the Reisz representation theorem shows that there exists a unique solution u in $H^1_{per}(Y \setminus R)/\mathbb{C}$ of

$$B_z(u,v) = \overline{F(v)}, \text{ for all } v \text{ in } H^1_{per}(Y \setminus R)/\mathbb{C}, \tag{2.4.6}$$

□

Chapter 3

Analysis on power series solution of cell problem

3.1 Effective properties and leading order dispersive effects

In this part we use the complete orthonormal systems of eigenfunctions associated with generalized electrostatic resonances and Dirichlet eigenvalues to explicitly solve for fields ψ_0 in Y and ψ_1 in $Y \setminus R$ and provide an explicit formula for ξ_0.

Applying the convention $\psi_m = 0$ for $m < 0$ in (2.1.8) shows that ψ_0 is the solution of

$$B_z(\psi_0, v) = 0, \text{ for all } v \text{ in } H^1(Y \setminus R). \tag{3.1.1}$$

From Theorem 2.2.1 and (2.2.1) we have the dichotomy:

1. ξ_0 satisfies $\epsilon_P^{-1}(\xi_0) = (\lambda_i + 1/2)/(\lambda_i - 1/2)$ and ψ_0 is an eigenfunction for (2.1.9).

2. ξ_0 satisfies $\epsilon_P^{-1}(\xi_0) \neq (\lambda_i + 1/2)/(\lambda_i - 1/2)$, $i = 1, 2, \ldots$ and $\psi_0 = \textit{constant}$.

In this article we assume the second alternative. Subsequent work will investigate the case when the first alternative is applied. For future reference the condition $\epsilon_P^{-1}(\xi_0) \neq (\lambda_i + 1/2)/(\lambda_i - 1/2)$ is equivalent to

$$\xi_0 \neq \zeta_i, \quad \zeta_i \equiv (\lambda_i + \tfrac{1}{2})\tfrac{\epsilon_r \omega_p^2}{c^2} \quad , 0 \leq \zeta_i \leq \frac{\epsilon_r \omega_p^2}{c^2} \; i = 1, 2, \ldots. \tag{3.1.2}$$

Restricting to test functions v with support in R in (2.1.8) we get

$$\int_R (\nabla \psi_0 \cdot \nabla \overline{v} - \xi_0 \psi_0 \overline{v}) \; d\mathbf{y} = 0. \tag{3.1.3}$$

From continuity we have the boundary condition for ψ_0 on R given by $\psi_0 = const.$ We denote the Dirichlet eigenvalues for R by ν_j, $j = 1, 2, \ldots$. Here we have the alternative:

1. If ξ_0 is a Dirichlet eigenvalue ν_i of $-\Delta$ in R then $\psi_0(\mathbf{y}) = 0$ for $\mathbf{y}$ in $Y \setminus R$.

2. If $\xi_0 \neq \nu_i$, $i = 1, 2, \ldots$ then ψ_0 is the unique solution of the Helmholtz equation (3.1.3) and $\psi_0 = const.$ in $Y \setminus R$.

In this treatment we will choose the second alternative $\xi_0 \neq \nu_i$. The case when the first alternative is chosen will be taken up in future investigation. Since $u_0 = \underline{u}_0\psi_0$ where $\underline{u}_0$ is an arbitrary constant we can without loss of generality make the choice $\psi_0 = 1$ for $\mathbf{y}$ in $Y \setminus R$. Since $\xi_0 \neq \nu_i$, $i = 1, \ldots$ and $\psi_0 = 1$ in $Y \setminus R$ a straight forward calculation gives ψ_0 in R in terms of the complete set of Dirichlet eigenfunctions and eigenvalues:

$$\psi_0 = \sum_{n=1}^{\infty} \frac{\mu_n < \phi_n >_R}{\mu_n - \xi_0} \phi_n, \text{ in } R. \tag{3.1.4}$$

Note here that μ_n denote the Dirichlet eigenvalues of $-\Delta$ in R whose eigenfunctions ϕ_n have nonzero mean, $< \phi_n >_R = \int_R \phi_n(y)dy \neq 0$. The Dirichlet eigenvalues associated with zero mean eigenfunctions are denoted by μ_n' and $\{\nu_n\}_{n=1}^{\infty} = \{\mu_n\}_{n=1}^{\infty} \cup \{\mu_n'\}_{n=1}^{\infty}$.

To find ψ_1 in $Y \setminus R$, we appeal to (2.1.8) with $\psi_0 = 1$ in $Y \setminus R$ to discover

$$B_z(\psi_1, v) = -\int_H \hat{\kappa} \cdot \nabla \overline{v} - \int_P \epsilon_P^{-1}(\xi_0)\hat{\kappa} \cdot \nabla \overline{v} \quad \forall \ \ v \in H^1_{per}(Y) \tag{3.1.5}$$

It follows from Theorem 2.2.2 that the problem has a unique solution subject to the mean-zero condition: $\int_{Y \setminus R} \psi_1 = 0$ provided that $\xi_0 \neq \zeta_i$, $i = 1, 2, \ldots$. We apply the decomposition of $H^1_{per}(Y \setminus R)/\mathbb{C}$ given by (2.2.1) and represent ψ_1 in terms of the complete set of orthonormal eigenfunctions $\{\psi_{\lambda_n}\} \subset W_3$ associated

with $-1/2 < \lambda_n < 1/2$ together with the complete orthonormal sets of functions for W_1 and W_2, denoted by $\{\psi_n^1\}_{n=1}^{\infty}$ and $\{\psi_n^2\}_{n=1}^{\infty}$ respectively. A straight forward calculation gives the representation for ψ_1 in $Y \setminus R$

$$\psi_1 = -\sum_{-\frac{1}{2}<\lambda_n<\frac{1}{2}} \left(\frac{(\alpha_{\lambda_n}^1 + \epsilon_P^{-1}(\xi_0)\alpha_{\lambda_n}^2)}{1 + (\epsilon_P^{-1}(\xi_0) - 1)(1 - \lambda_n)} \right) \psi_{\lambda_n} + \sum_{n=1}^{\infty} \alpha_{1,n}\psi_n^1 \text{ in } Y \setminus R \quad (3.1.6)$$

with

$$\begin{aligned} &\alpha_{\lambda_n}^1 = \hat{\kappa} \cdot \int_H \nabla\psi_{\lambda_n}\, d\mathbf{y},\ \alpha_{\lambda_n}^2 = \hat{\kappa} \cdot \int_P \nabla\psi_{\lambda_n}\, d\mathbf{y}, \\ &\text{and } \alpha_{1,n} = \hat{\kappa} \cdot \int_H \nabla\psi_n^1\, d\mathbf{y}. \end{aligned} \quad (3.1.7)$$

Setting $v = 1$ and $m = 2$ in (2.1.8) we recover the solvability condition given by

$$\begin{aligned} &\tau^2 \int_{H\cup P} \big[-\hat{\kappa} \cdot \xi_0 \nabla\psi_1 + \xi_0 \big] - \tau^2 \epsilon_r \frac{\omega_p^2}{c^2} \int_H (-\hat{\kappa}\nabla\psi_1 + 1) \quad (3.1.8) \\ &= \int_Y (\xi_0^2\psi_0 - \epsilon_r \frac{\omega_p^2}{c^2}\xi_0\psi_0) \end{aligned}$$

Substitution of the spectral representations for ψ_1 and ψ_0 given by (3.1.4) and (3.1.6) into (3.1.8) delivers the quasistatic dispersion relation

$$\xi_0 = \tau^2 n_{eff}^{-2}(\xi_0), \quad (3.1.9)$$

where the effective index of diffraction n_{eff}^2 depends upon the direction of propagation $\hat{\kappa}$ and is written

$$n_{eff}^2(\xi_0) = \mu_{eff}(\xi_0)/\epsilon_{eff}^{-1}(\xi_0)\hat{\kappa} \cdot \hat{\kappa}. \quad (3.1.10)$$

The frequency dependent effective magnetic permeability μ_{eff} and effective dielectric permittivity ϵ_{eff} are given by

$$\mu_{eff}(\xi_0) = \int_Y \psi_0 = \theta_H + \theta_P + \sum_{n=1}^{\infty} \frac{\mu_n < \phi_n >_R^2}{\mu_n - \xi_0} \quad (3.1.11)$$

and

$$\begin{aligned}
&\epsilon_{eff}^{-1}(\xi_0)\hat{\kappa}\cdot\hat{\kappa} \\
&\quad = \int_H (I-\mathbb{P})\hat{\kappa}\cdot\hat{\kappa}\,d\mathbf{y} + \frac{\xi_0}{\xi_0 - \frac{\epsilon_r\omega_p^2}{c^2}}\theta_P \qquad (3.1.12)\\
&\quad - \sum_{-\frac{1}{2}<\lambda_h<\frac{1}{2}} \left(\frac{\left(\xi_0 - \frac{\epsilon_r\omega_p^2}{c^2}\right)|\alpha_{\lambda_h}^{(1)}|^2 + 2\frac{\epsilon_r\omega_p^2}{c^2}\alpha_{\lambda_h}^{(1)}\alpha_{\lambda_h}^{(2)} + \frac{\left(\frac{\epsilon_r\omega_p^2}{c^2}\right)^2}{\xi_0 - \frac{\epsilon_r\omega_p^2}{c^2}}|\alpha_{\lambda_h}^{(2)}|^2}{\xi_0 - s_h} \right),
\end{aligned}$$

where θ_H and θ_P are the areas occupied by regions H and P respectively. The first term on the right hand side of (3.1.12) is positive and frequency independent. It is written in terms of the spectral projection $\mathbb{P}$ of square integrable vector fields over H onto the subspace of gradients of potentials ψ in $H^1_{0,per}(H)$. Here $\int_H \mathbb{P}\hat{\kappa}\cdot\hat{\kappa}\,d\mathbf{y} < \theta_H$ and $\mathbb{P}\sigma = \sum_{n=1}^{\infty}\left(\int_H \nabla\psi_n^1\cdot\sigma\,d\mathbf{y}\right)\nabla\psi_n^1$ with $\sum_{n=1}^{\infty}|\alpha_{1,n}|^2 = \int_H \mathbb{P}\hat{\kappa}\cdot\hat{\kappa}\,d\mathbf{y}$. The poles s_h are the subset of values ζ_h for which at least one of the weights $\alpha_{\lambda_h}^{(1)}$ and $\alpha_{\lambda_h}^{(2)}$ are non zero. The values of ζ_h for which both weights vanish are denoted by s_h' and $\{\zeta_h\}_{h=1}^{\infty} = \{s_h\}_{h=1}^{\infty}\cup\{s_h'\}_{h=1}^{\infty}$. The graphs of μ_{eff} and $\epsilon_{eff}^{-1}\hat{\kappa}\cdot\hat{\kappa}$ as functions of ξ_0 are displayed in Figure 3.1 and Figure 3.2. Here the intervals $a' < \xi_0 < b'$ and $a'' < \xi_0 < b''$ are the same in all graphs.

For future reference is is convenient to write the dispersion relation explicitly in terms of μ_{eff} and ϵ_{eff} and

$$\mu_{eff}(\xi_0)\xi_0 = \tau^2\epsilon_{eff}^{-1}(\xi_0)\hat{\kappa}\cdot\hat{\kappa}. \qquad (3.1.13)$$

The branches of the quasistatic dispersion relation $(\tau,\hat{\kappa})\mapsto\xi_0$ are controlled by the poles and zeros of μ_{eff} and ϵ_{eff}^{-1} explicitly determined through the Dirichlet spectra and generalized electrostatic resonances.

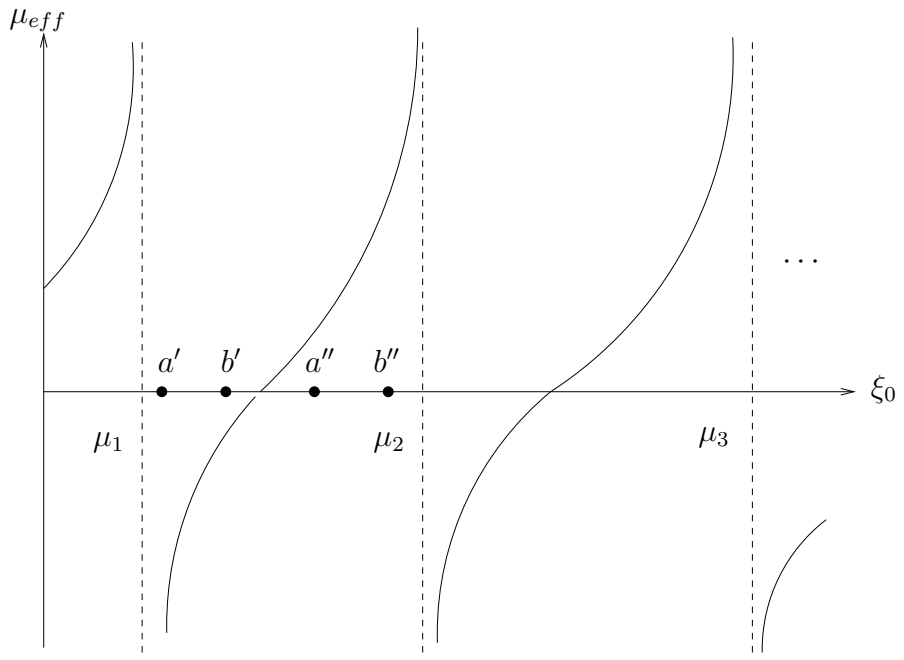

FIGURE 3.1: The relation between μ_{eff} and ξ_0.

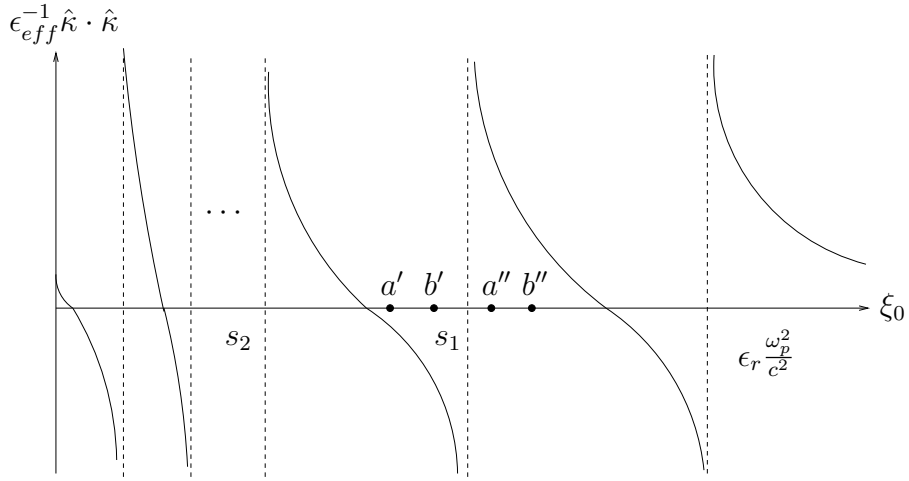

FIGURE 3.2: The relation between $\epsilon_{eff}^{-1}\hat{\kappa}\cdot\hat{\kappa}$ and ξ_0.

3.2 Solution of higher order problems

Having determined ψ_0 in Y, ψ_1 in $Y \setminus R$, and ξ_0, we now provide the algorithm for determining the rest of the elements in the sequences $\{\psi_m\}_{m=0}^{\infty}$, $\{\xi_m\}_{m=0}^{\infty}$ for the infinite set of coupled equations (2.1.8) and show that the boundary value problems used to determine ψ_m in $Y \setminus R$, $m \geq 2$ and ψ_m in R for $m \geq 1$ together

with solvability conditions for ξ_m for $m \geq 1$ are a well posed infinite system of equations. The algorithm is summarized in Theorem 3.2.1.

Step I. *Solution of ψ_m in R for $m \geq 1$.*

We restrict the trial space to test functions v with support in R and put $m \mapsto m+2$ in (2.1.8). We decompose ψ_m according to

$$\psi_m = \tilde{\psi}_m + (-i)^m \xi_m \psi_* \tag{3.2.1}$$

and substitute into (2.1.8). This decomposition is chosen such that $\tilde{\psi}_m$ depends on ξ_n and ψ_n inside R for $n \leq m-1$. The function ψ_* depends only upon ξ_0 and ψ_0 in R. The function $\tilde{\psi}_m$ solves the Dirichlet boundary value problem with $\tilde{\psi}_m|_{\partial R-} = \psi_m|_{\partial R+}$ and

$$\int_R \left(\nabla \tilde{\psi}_m \cdot \nabla \overline{v} - \xi_0 \tilde{\psi}_m \overline{v} \right) \, d\mathbf{y} = \int_R F \cdot \nabla \overline{v} \, d\mathbf{y} + \int_R G \overline{v} \, d\mathbf{y}, \tag{3.2.2}$$

where

$$\begin{aligned} F &= -\xi_0^{-1} \epsilon_p^{-1}(\xi_0) [\sum_{l=1}^{m-1} (-i)^l \xi_l \nabla \psi_{m-l} + \hat{\kappa} (\sum_{l=0}^{m-1} (-i)^l \xi_l \psi_{m-1-l})] \\ &\quad + \xi_0^{-1} \epsilon_p^{-1}(\xi_0) \epsilon_r \frac{\omega_p^2}{c^2} \hat{\kappa} \psi_{m-1}, \end{aligned} \tag{3.2.3}$$

and

$$\begin{aligned} G &= \xi_0^{-1} \epsilon_p^{-1}(\xi_0) (\hat{\kappa} \cdot \sum_{l=0}^{m-1} (-i)^l \xi_l \nabla \psi_{m-1-l} + \sum_{l=0}^{m-2} (-i)^l \xi_l \psi_{m-2-l}) \\ &\quad - \xi_0^{-1} \epsilon_p^{-1}(\xi_0) (\hat{\kappa} \cdot \nabla \psi_{m-1} + \psi_{m-2}) \\ &\quad + \xi_0^{-1} \epsilon_p^{-1}(\xi_0) [\sum_{l=1}^{m-1} \sum_{n=0}^{l} \xi_{m-l} \xi_n \psi_{l-n} i^{l-n-m} \\ &\quad - \epsilon_r \frac{\omega_p^2}{c^2} \sum_{l=1}^{m-1} (-i)^l \xi_l \psi_{m-l} + \xi_0 \sum_{n=1}^{m-1} \xi_n \psi_{m-n} i^{-n}]. \end{aligned} \tag{3.2.4}$$

This boundary value problem has a unique solution for $\xi_0 \neq \nu_i$, $i = 1, \ldots$. The function ψ_* is the solution of

$$\begin{cases} \int_R (-\nabla\psi_* \cdot \nabla\overline{v} + \xi_0\psi_*\overline{v}) + \int_R \psi_0\overline{v} = 0 \\ \psi_*|_{\partial R-} = 0 \end{cases} \tag{3.2.5}$$

The explicit representation for ψ_* is obtained using the Dirichlet eigenfunctions on R and is given by,

$$\psi_* = \sum_{n=1}^{\infty} \frac{\mu_n < \phi_n >_R}{(\mu_n - \xi_0)^2}\phi_n \quad \text{in } R. \tag{3.2.6}$$

Step II. *Solution of ψ_m in $Y \setminus R$ for $m \geq 2$.*

We decompose ψ_m

$$\psi_m = \psi'_m + (-i)^{m-1}\xi_{m-1}\hat{\psi} \tag{3.2.7}$$

and substitute into (2.1.8). This decomposition is chosen such that ψ'_m depends on ξ_n for $0 \leq n \leq m-2$, the functions ψ_n, $n \leq m-1$ in $Y \setminus R$ and the functions ψ_n, $n \leq m-2$ in R. The function $\hat{\psi}$ depends only on ξ_0 and ψ_1 in $Y \setminus R$.

For $m \geq 2$, ψ'_m in $Y \setminus R$ subject to the mean zero condition $\int_{Y\setminus R} \psi'_m \, dy = 0$ is the solution of

$$\begin{aligned} \tau^2 B_z(\psi'_m, v) &= \int_{Y\setminus R} (F_1 \cdot \nabla\overline{v} + G_1\overline{v}) \, d\mathbf{y} \\ &\quad + \int_R (F_2 \cdot \nabla\overline{v} + G_2\overline{v}) \, d\mathbf{y}, \text{ for all } v \text{ in } H^1_{per}(Y), \end{aligned} \tag{3.2.8}$$

where

$$\begin{aligned} F_1 &= \xi_0^{-1}\epsilon_p^{-1}(\xi_0)\tau^2\big[\sum_{l=1}^{m-2}(-i)^l\xi_l\nabla\psi_{m-l} + (\sum_{l=0}^{m-2}(-i)^l\xi_l\psi_{m-1-l})\hat{\kappa}\big] \\ &\quad -\xi_0^{-1}\epsilon_p^{-1}(\xi_0)\tau^2\epsilon_r\frac{\omega_p^2}{c^2}\chi_H\hat{\kappa}\psi_{m-1}, \end{aligned} \tag{3.2.9}$$

$$
\begin{aligned}
G_1 &= \xi_0^{-1}\epsilon_p^{-1}(\xi_0)\tau^2\big[\hat{\kappa}\cdot\sum_{l=0}^{m-2}(-i)^l\xi_l(-\nabla\psi_{m-1-l}) - \sum_{l=0}^{m-2}(-i)^l\xi_l\psi_{m-2-l}\big] \\
&\quad -\xi_0^{-1}\epsilon_p^{-1}(\xi_0)\tau^2\epsilon_r\frac{\omega_p^2}{c^2}\chi_H\big[\hat{\kappa}\cdot(-\nabla\psi_{m-1}) - \psi_{m-2}\big] \\
&\quad +\xi_0^{-1}\epsilon_p^{-1}(\xi_0)\big[\sum_{l=0}^{m-2}\sum_{n=0}^{l}\xi_{m-2-l}\xi_n\psi_{l-n}i^{l-n-m} \\
&\quad -\epsilon_r\frac{\omega_p^2}{c^2}\sum_{l=0}^{m-2}(-i)^l\xi_l\psi_{m-2-l}\big], \qquad (3.2.10)
\end{aligned}
$$

$$
\begin{aligned}
F_2 &= -\xi_0^{-1}\epsilon_p^{-1}(\xi_0)\big[\sum_{l=0}^{m-2}(-i)^l\xi_l\nabla\psi_{m-2-l} + \hat{\kappa}(\sum_{l=0}^{m-3}(-i)^l\xi_l\psi_{m-3-l})\big] \\
&\quad +\xi_0^{-1}\epsilon_p^{-1}(\xi_0)\epsilon_r\frac{\omega_p^2}{c^2}\big[\nabla\psi_{m-2} + \hat{\kappa}(\psi_{m-3})\big], \qquad (3.2.11)
\end{aligned}
$$

and

$$
\begin{aligned}
G_2 &= -\xi_0^{-1}\epsilon_p^{-1}(\xi_0)\big[+ \hat{\kappa}(\sum_{l=0}^{m-3}(-i)^l\xi_l(-\nabla\psi_{m-3-l})) \\
&\quad -\sum_{l=0}^{m-4}(-i)^l\xi_l\psi_{m-4-l}\big] + \xi_0^{-1}\epsilon_p^{-1}(\xi_0)\epsilon_r\frac{\omega_p^2}{c^2}\big[\hat{\kappa}\cdot(-\nabla\psi_{m-3}) + \psi_{m-4}\big] \\
&\quad +\xi_0^{-1}\epsilon_p^{-1}(\xi_0)\big[\sum_{l=0}^{m-2}\sum_{n=0}^{l}\xi_{m-2-l}\xi_n\psi_{l-n}i^{l-n-m}\overline{v} \\
&\quad -\epsilon_r\frac{\omega_p^2}{c^2}\sum_{l=0}^{m-2}(-i)^l\xi_l\psi_{m-2-l}\overline{v}\big], \qquad (3.2.12)
\end{aligned}
$$

where χ_H is the indicator function of the host domain H taking 1 inside and zero outside. Here we have used the identity $\psi_0(\mathbf{y}) = 1$, for $\mathbf{y} \in Y \setminus R$ in determining the formulas for the right hand side of (3.2.8).

Setting $v = 1$ in (3.2.8) delivers the solvability condition

$$
\int_{Y\setminus R} G_1\, d\mathbf{y} + \int_R G_2\, d\mathbf{y} = 0. \qquad (3.2.13)
$$

The condition

$$
-\nabla\cdot F_2 + G_2 = 0 \text{ for } \mathbf{y} \text{ in } R \qquad (3.2.14)
$$

follows from the solution of Step I see, (3.2.1), (3.2.2) and (3.2.5). Integration by parts on the left hand side of (3.2.8) together with (3.2.14) transforms (3.2.8) into the equivalent Neumann boundary value problem for ψ'_m, $m \geq 2$, given by

$$\begin{aligned} \tau^2 B_z(\psi'_m, v) &= \int_{Y\setminus R} (F_1 \cdot \nabla \overline{v} + G_1 \overline{v})\, d\mathbf{y} \\ &\quad + \int_{\partial R} F_2 \cdot n \overline{v}\, ds, \text{ for all } v \text{ in } H^1_{per}(Y \setminus R), \end{aligned} \tag{3.2.15}$$

where n is the outward directed unit normal to ∂R. Finally we observe that the solvability condition for the Neumann problem (3.2.15) given by

$$\int_{Y\setminus R} G_1\, d\mathbf{y} + \int_{\partial R} F_2 \cdot n\, ds = 0, \tag{3.2.16}$$

follows immediately from (3.2.13) and (3.2.14). This Neumann problem satisfies the hypotheses of Theorem 2.2.2 and we assert the existence of a solution ψ'_m for (3.2.15), uniquely determined by the condition $\int_{Y\setminus R} \psi'_m\, dy = 0$, provided that $\xi_0 \neq \zeta_i$, $0 \leq \zeta_i \leq \frac{\epsilon_r \omega_P^2}{c^2}$, $i = 1, 2, \ldots$.

The field $\hat{\psi}$ solves

$$\begin{cases} B_z(\hat{\psi}, v) = -\xi_0^{-1} \epsilon_p^{-1}(\xi_0) \int_{Y\setminus R} (\nabla \psi_1 + \hat{\kappa}) \cdot \nabla \overline{v}, \\ \int_{Y\setminus R} \hat{\psi} = 0, \end{cases} \tag{3.2.17}$$

for all trials $v \in H^1_{per}(Y \setminus R)$. The solution $\hat{\psi}$ is represented explicitly in terms of the eigenvectors associated with the generalized electrostatic resonances. A straight forward calculation gives

$$\hat{\psi} = \sum_{-\frac{1}{2}<\lambda_n<\frac{1}{2}} \frac{\psi_{\lambda_n}}{\xi_0 - (\frac{1}{2}+\lambda_n)\frac{\epsilon_r \omega_p^2}{c^2}} \left(-(\alpha^1_{\lambda_n} + \alpha^2_{\lambda_n}) + \frac{(\xi_0 - \frac{\epsilon_r \omega_p^2}{c^2})\left(\alpha^1_{\lambda_n} + \alpha^2_{\lambda_n}\left(\frac{\xi_0}{\xi_0 - \frac{\epsilon_r \omega_p^2}{c^2}}\right)\right)}{\xi_0 - s_i} \right). \tag{3.2.18}$$

Step III. *Solution of ξ_m for $m \geq 1$.*

We apply the decomposition (3.2.1) to ψ_{m-2} in R and (3.2.7) to ψ_{m-1} in $Y \setminus R$. Substitution of the decompositions into the solvability condition (3.2.13) and applying the explicit spectral representations (3.2.6), (3.2.18) for ψ_* and $\hat{\psi}$ we obtain the recursion relation for determining $\xi_1, \xi_2, \ldots$ given by

$$\begin{aligned}
\xi_{m-2}\mathcal{G}(\xi_0) &= \tau^2 \int_{Y\setminus R} \big[\hat{\kappa}\cdot(\sum_{l=1}^{m-3}(-i)^l\xi_l\nabla\psi_{m-1-l} + \xi_0\nabla\psi'_{m-1}) \\
&+ \sum_{l=0}^{m-3}(-i)^l\xi_l\psi_{m-2-l}\big] - \tau^2\int_H \epsilon_r\frac{\omega_p^2}{c^2}(\hat{\kappa}\cdot\nabla\psi'_{m-1} + \psi_{m-2}) \\
&- \int_R \big[\hat{\kappa}\cdot\sum_{l=0}^{m-3}(-i)^l\xi_l\nabla\psi_{m-3-l} + \sum_{l=0}^{m-4}(-i)^l\xi_l\psi_{m-4-l}\big] \\
&- \int_Y \big[\sum_{l=1}^{m-3}\sum_{n=0}^{l} i^{l-n-m}\xi_{m-2-l}\xi_n\psi_{l-n} - \sum_{l=1}^{m-3}(-i)^l\xi_0\xi_l\psi_{m-2-l}\big] \\
&- \int_R \xi_0^2\tilde{\psi}_{m-2} - \int_{Y\setminus R}\xi_0^2\psi_{m-2} + \int_Y \epsilon_r\frac{\omega_p^2}{c^2}\sum_{l=1}^{m-3}(-i)^l\xi_l\psi_{m-2-l} \\
&+ \int_R \epsilon_r\frac{\omega_p^2}{c^2}\xi_0\tilde{\psi}_{m-2} + \int_{Y\setminus R}\epsilon_r\frac{\omega_p^2}{c^2}\xi_0\psi_{m-2}. \qquad (3.2.19)
\end{aligned}$$

Noting that (3.2.1) and (3.2.7) can also be applied to the lower order terms on the right hand side of (3.2.19) we see that (3.2.19) determines ξ_{m-2} from ξ_n, ψ_n in $Y \setminus R$, and ψ_n in R with $0 \leq n \leq m-3$. Here the "solvability matrix," $\mathcal{G}$ depends explicitly on ξ_0 and is given by

$$\begin{aligned}
&\mathcal{G}(\xi_0) = \theta_H + \theta_P \\
&+\tau^2\big[\int_H \mathbb{P}\hat{\kappa}\cdot\hat{\kappa}\,d\mathbf{y} - \sum_{n=1}^{\infty}(g_n^2(\xi_0)|\alpha^1_{\lambda_n} + \epsilon_P^{-1}(\xi_0)\alpha^2_{\lambda_n}|^2) \\
&+2g_n(\xi_0)(\alpha^1_{\lambda_n} + \alpha^2_{\lambda_n})(\alpha^1_{\lambda_n} + \epsilon_P^{-1}(\xi_0)\alpha^2_{\lambda_n})\big] \\
&-2(\xi_0 + \frac{\epsilon_r\omega_p^2}{c^2})\mu_{eff}(\xi_0) + \xi_0(\xi_0 - \frac{\epsilon_r\omega_p^2}{c^2})\sum_{n=1}^{\infty}\frac{\mu_n\langle\phi_n\rangle_R^2}{(\mu_n - \xi_0)^2}, \qquad (3.2.20)
\end{aligned}$$

where $g_n(\xi_0) = (\xi_0 - \frac{\epsilon_r\omega_p^2}{c^2})/(\xi_0 - s_n)$ and $\epsilon_P^{-1}(\xi_0) = \xi_0/(\xi_0 - \frac{\epsilon_r\omega_p^2}{c^2})$. The set of poles and zeros for $\mathcal{G}(\xi_0)$ are explicitly controlled by the generalized electrostatic

resonances and Dirichlet spectra. The zeros of $\mathcal{G}$ are denoted by γ_n, $n = 1, \ldots$. It is now evident that the recursion relation (3.2.19) holds provided that $\xi_0 \neq \nu_n$, $\xi_0 \neq \zeta_n$, and $\xi_0 \neq \gamma_n$.

Denote the union of the Dirichlet spectra, the electrostatic resonances, and zeros of $\mathcal{G}$ by

$$U \equiv \{\nu_j\}_{j=1}^{\infty} \cup \{\zeta_j\}_{j=1}^{\infty} \cup \{\gamma_j\}_{j=1}^{\infty} \tag{3.2.21}$$

where $\{\nu_j\}_{j=1}^{\infty} \subset \mathbb{R}^+$, $\{\gamma_j\}_{j=1}^{\infty} \subset \mathbb{R}^+$, and $\{\zeta_j\}_{j=1}^{\infty} \subset [0, \frac{\epsilon_r \omega_p^2}{c^2}]$. We collect results and state the following theorem.

Theorem 3.2.1. *If ξ_0 belongs to $\mathbb{R}^+ \setminus U$ then the sequences $\{\psi_m\}_{m=0}^{\infty} \subset H^1_{per}(Y)$, $\{\xi_m\}_{m=0}^{\infty} \subset \mathbb{C}$ exist and are uniquely determined.*

Proof. The functions ψ_0 in $H^1(Y)$ and ψ_1 in $H^1(Y \setminus R)$ with $\int_{Y \setminus R} \psi_1 \, dy = 0$ exist as does ξ_0. Application of Step I uniquely determines $\tilde{\psi}_1$ in R. Application of Step II uniquely determines ψ_2' in $Y \setminus R$. Step III uniquely determines ξ_1 and we apply (3.2.1) and (3.2.7) to recover ψ_1 in $H^1(Y)$ and ψ_2 in $H^1(Y \setminus R)$ with $\int_{Y \setminus R} \psi_2 \, dy = 0$.

We now adopt the induction hypotheses H_n, $n \geq 2$:

There exist

1) $\psi_n \in H^1_{per}(Y \setminus R)$ with $\int_{Y \setminus R} \psi_n = 0$;

2) $\psi_j \in H^1_{per}(Y)$ for $0 \leq j \leq n-1$ with $\int_{Y \setminus R} \psi_j = 0$, $1 \leq j \leq n-1$;

3) $\xi_{n-1} \in \mathbb{C}$.

Application of Step I uniquely determines $\tilde{\psi}_n$ in R. Application of Step II uniquely determines ψ_{n+1}' in $Y \setminus R$. Step III uniquely determines ξ_n and we apply (3.2.1) and (3.2.7) to recover ψ_n in $H^1(Y)$ and ψ_{n+1} in $H^1(Y \setminus R)$ with $\int_{Y \setminus R} \psi_{n+1} \, dy = 0$. $\square$

3.3 Band structure for the metamaterial crystal and main theorems

In this part we present explicit formulas describing the band structure for the metamaterial crystal in the dynamic, sub-wavelength regime $1 > \eta > 0$. The formulas show that the frequency intervals associated with pass bands and stop bands are governed by the poles and zeros of the effective magnetic permittivity and dielectric permittivity tensors. The poles and zeros are explicitly determined by the Dirichlet spectra of R and the generalized electrostatic resonances of $Y \setminus R$, see (3.1.11) and (3.1.12). For the general class of parallel rod configurations treated here the pass bands and stop bands can exhibit anisotropy, i.e., dependence on the direction of propagation described by $\hat{\kappa}$. The anisotropy is governed by the projection of $\hat{\kappa}$ onto the eigenfunctions associated with the generalized electrostatic resonances given by (3.1.7). In what follows pass bands are explicitly linked to frequency intervals and propagation directions for which both the effective magnetic permittivity and dielectric permeability have the same sign. This includes frequency intervals where effective tensors are either simultaneously positive or negative.

We begin by identifying the locations of the branches for the dispersion relation associated with the metamaterial crystal. We introduce the union of open intervals $\bigcup_n O_n$ on the positive real axis $\mathbb{R}^+$ obtained by removing the points $\{\zeta_j\}_{j=1}^{\infty}$, $\{\nu_j\}_{j=1}^{\infty}$, $\{\gamma_j\}_{j=1}^{\infty}$, $\{s_j^*\}_{j=1}^{\infty}$ and $\{\mu_j^*\}_{j=1}^{\infty}$. Here s_j^* is the zero of $\epsilon_{eff}^{-1}(\xi_0)\hat{\kappa}\cdot\hat{\kappa}$ between s_j and s_{j+1} and μ_j^* is the zero of $\mu_{eff}(\xi_0)$ between μ_j and μ_{j+1}. The leading order dispersion relation (3.1.13) implicitly defines the map $(\tau, \hat{\kappa}) \mapsto \xi_0$. We denote the branch associated with O_n by $\xi_0^n = \xi_0^{(n)}(\tau, \hat{\kappa})$. Let I_n be an open interval strictly contained inside O_n. For this choice $I_n \subset O_n$ does not intersect the union of the Dirichlet spectra, generalized electrostatic spectra and the zeros of the solvability matrix $\mathcal{G}$, see (3.2.21).

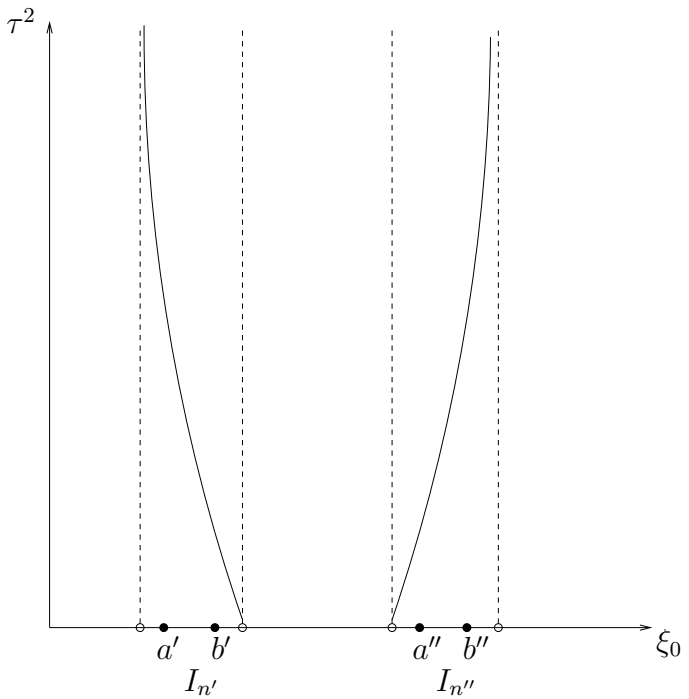

FIGURE 3.3: The leading order dispersion relation over two selected intervals $I_{n'}$ and $I_{n''}$.

The band structure for the metamaterial in the dynamic sub-wavelength regime $1 > \eta > 0$ is given by the following theorem.

Theorem 3.3.1. *The dispersion relation for the metamaterial crystal contains an infinite sequence of branches with leading order behavior given by the functions* $\xi_0^n = \xi_0^n(\tau, \hat{\kappa})$. *For* τ *such that* ξ_0^n *belongs to* I_n *there exists a constant* R *depending only on* I_n *such that for* $0 < \rho < R$, *the branch of the dispersion relation for the metamaterial crystal is given by*

$$\xi^n = \xi_0^n(\tau, \hat{\kappa}) + \sum_{l=1}^{\infty} (\rho\tau)^l \xi_l^n, \tag{3.3.1}$$

for

$$\{-2\pi \leq \tau\rho\hat{\kappa}_1 \leq 2\pi, -2\pi \leq \tau\rho\hat{\kappa}_2 \leq 2\pi\}. \tag{3.3.2}$$

Here the higher order terms ξ_l^n *are real and are uniquely determined by* ξ_0^n *according to Theorem 3.2.1.*

The power series representation for the transverse magnetic Bloch wave (1.2.2) is given by the following theorem.

Theorem 3.3.2. *For I_n and R as in Theorem 3.3.1 and for τ such that ξ_0^n belongs to I_n there exist transverse magnetic Bloch waves given by the expansion*

$$H_3^n = \underline{u}_0 \left(\psi_0(\boldsymbol{x}/d) + \sum_{l=1}^{\infty} (\rho\tau)^l i^l \psi_l(\boldsymbol{x}/d) \right) exp\left\{ i\left(k\hat{\kappa}\cdot\boldsymbol{x} - t\frac{\omega}{c} \right) \right\}, \tag{3.3.3}$$

where the series

$$\psi_0(\boldsymbol{y}) + \sum_{l=1}^{\infty} (\rho\tau)^l i^l \psi_l(\boldsymbol{y}) \tag{3.3.4}$$

is summable in $H^1(Y)$ for $0 \le \rho < R$ and $\frac{\omega}{c} = \sqrt{\frac{\xi^n}{\epsilon_r}}$.

Theorem 3.3.1 explicitly shows that the leading order behavior determines the existence of pass bands or stop bands when $\rho = d/\sqrt{\epsilon_r}$ is sufficiently small. With this in mind we can appeal to (3.1.13) and state the following theorem.

Theorem 3.3.3. *For $\rho > 0$ sufficiently small:*

- *There exist propagating Bloch wave solutions along directions $\hat{\kappa}$ over intervals I_n for which $\mu_{eff}(\xi_0^n)$ and $\epsilon_{eff}^{-1}(\xi_0^n)\hat{\kappa}\cdot\hat{\kappa}$ have the same sign.*
- *Intervals I_n for which $\mu_{eff}(\xi_0^n)$ and $\epsilon_{eff}^{-1}(\xi_0^n)\hat{\kappa}\cdot\hat{\kappa}$ have the opposite sign lie within stop bands.*

Leading order behavior for pass bands associated with double negative and double positive behavior are illustrated in Figure 3.3 for two intervals $I_{n'}$ and $I_{n''}$. Here the effective properties are both negative over the interval $I_{n'}$ while they are both positive over $I_{n''}$.

3.4 Convergence of the power series

In this part we show that the series (3.3.1), (3.3.4) identified in Theorems 3.3.1 and 3.3.2 are convergent. Here the convergence radius R depends upon the branch

of the quasistatic dispersion relation $\xi_0^n = \xi_0^n(\tau, \hat{\kappa})$. The methodology applied here uses generating functions and follows the approach presented in [21].

Step I. *A priori estimates.*

We establish a priori bounds for the solutions of (3.2.2) and (3.2.15). Before proceeding recall the Friderich's inequality and trace estimate satisfied by elements ψ of $H^1_{per}(Y \setminus R)/\mathbb{C}$ given by

$$\|\psi\|_{Y\setminus R} = \left(\int_{Y\setminus R} |\nabla\psi|^2 + |\psi|^2\, dy\right)^{1/2} \leq \Omega\|\psi\| \tag{3.4.1}$$

and

$$\|\psi\|_{H^{1/2}(\partial R)} \leq A\|\psi\| \tag{3.4.2}$$

where Ω and A are positive constants depending on R and $\|\psi\|$ is the norm on $H^1_{per}(Y \setminus R)/\mathbb{C}$ defined by (2.1.2).

The solutions $\tilde{\psi}$ of (3.2.2) solve boundary value problems of the following generic form. Given $\psi \in H^1_{per}(Y \setminus R)$, $G \in L^2(R)$ and $F \in [L^2(R)]^2$ the function $\tilde{\psi}$ is the $H^1(R)$ solution of

$$\begin{cases} \int_R(\nabla\tilde{\psi}\cdot\nabla\overline{v} - \xi_0\psi\overline{v}) = \int_R G\overline{v} + \int_R F\cdot\nabla\overline{v} \qquad \forall v \in H^1_0(R) \\ \tilde{\psi}|_{\partial R-} = \psi|_{\partial R+}. \end{cases} \tag{3.4.3}$$

Decompose $\tilde{\psi}$ according to $\tilde{\psi} = \psi_0 + \psi_1 + \psi_2$ such that

$$\begin{cases} \int_R(\nabla\psi_0\cdot\nabla\overline{v} - \xi_0\psi_0\overline{v}) = \int_R [G + (1+\xi_0)\psi_1 + (1+\xi_0)\psi_2]\,\overline{v} \qquad \forall v \in H^1_0(R) \\ \psi_0|_{\partial R-} = 0, \end{cases} \tag{3.4.4}$$

$$\begin{cases} \int_R(\nabla\psi_1\cdot\nabla\overline{v} + \psi_1\overline{v}) = 0 \qquad \forall v \in H^1_0(R) \\ \psi_1|_{\partial R-} = \psi|_{\partial R+}, \end{cases} \tag{3.4.5}$$

and

$$\begin{cases} \int_R (\nabla\psi_2 \cdot \nabla\overline{v} + \psi_2\overline{v}) = \int_R F \cdot \nabla\overline{v} \qquad \forall v \in H_0^1(R) \\ \psi_2|_{\partial R-} = 0. \end{cases} \tag{3.4.6}$$

Let $J = G+(1+\xi_0)\psi_1+(1+\xi_0)\psi_2$ denote the right hand side for (3.4.4). Expanding ψ_0 and J with respect to the complete orthonormal set of Dirichlet eigenfunctions $\{\phi_j\}_{j=1}^{\infty}$, $\{\nu_j\}_{j=1}^{\infty}$ gives

$$\|\psi_0\|^2_{H^1(R)} = \sum_{j=1}^{\infty}(1+\nu_j)\left|\frac{\langle J\psi_j\rangle_R}{(\xi_0-\nu_j)}\right|^2 \leq C^2_{1,n}\|J\|^2_{L^2(R)}, \tag{3.4.7}$$

where

$$C_{1,n} = \max_{\xi_0\in I_n}\left\{max_j\left\{\frac{(1+\nu_j)^{1/2}}{|\xi_0-\nu_j|}\right\}\right\}. \tag{3.4.8}$$

Collecting results gives

$$\begin{aligned} ||\psi_1||_{H^1(R)} &= ||\psi_2||_{H^{1/2}(\partial R)} \leq A||\psi|| \\ ||\psi_2||_{H^1(R)} &\leq ||F||_{L^2(R)} \\ ||\psi_0||_{H^1(R)} &\leq C_{1,n}||G+(1+\xi)\psi_1+(1+\xi)\psi_2||_{L^2(R)} \end{aligned} \tag{3.4.9}$$

and

$$||\tilde{\psi}||_{H^1(R)} \leq B_n(||G||_{L^2(R)} + ||F||_{L^2(R)} + ||\psi||), \tag{3.4.10}$$

where

$$B_n = max_{\xi_0\in I_n}\{C_{1,n}, C_{1,n}(1+\xi_0), A(C_{1,n}(1+\xi_0)+1)\}. \tag{3.4.11}$$

Now we estimate the field ψ_*. The explicit expression (3.2.6) for ψ_* gives

$$||\psi_*||^2_{H^1(R)} = \sum_{n=1}^{\infty}\frac{(1+\mu_n)\mu_n^2 < \phi_n >^2_R}{(\mu_n-\xi_0)^4}, \tag{3.4.12}$$

and

$$||\psi_*||_{H^1(R)} \leq L_n. \tag{3.4.13}$$

where L_n is the maximum of the right hand side of (3.4.12) for $\xi_0(\tau,\hat{\kappa}) \in I_n$.

Next we provide an upper bound for the solutions of ψ'_m of (3.2.15). We may continuously extend elements v in $H^1_{per}(Y\setminus R)/\mathbb{C}$ onto R as $H^1_{per}(Y)$ functions such that the extension v^{ext} satisfies

$$\|v^{ext}\|_Y \leq C\|v\|. \tag{3.4.14}$$

In what follows we continue to denote these extensions by v and (3.2.15) takes the equivalent form (3.2.8). Application of Hölders inequality to the right hand side of (3.2.8) gives

$$\begin{aligned} \tau^2|B_z(\psi'_m,v)| &= C(||F_1||_{L^2(Y\setminus R)}+||G_1||_{L^2(Y\setminus R)} \\ &\quad +||F_2||_{L^2(R)}+||G_2||_{L^2(R)})||v||. \end{aligned} \tag{3.4.15}$$

It is evident that $B_z(\psi'_m,\psi'_m)=(T_z\psi'_m,\psi'_m)$ and applying the explicit representation for T_z delivers the estimate

$$\begin{aligned} \tau^2\|\psi'_m\|^2 &\leq G_z\tau^2|B(\psi'_m,\psi'_m)| \\ &\leq C\times G_z(||F_1||_{L^2(Y\setminus R)}+||G_1||_{L^2(Y\setminus R)} \\ &\quad +||F_2||_{L^2(R)}+||G_2||_{L^2(R)})||v||, \end{aligned} \tag{3.4.16}$$

with

$$G_z=(\min\{1,|z|,\inf_{-1/2<\lambda_n<1/2}\{|1+(z-1)(1/2-\lambda_n)|\}\})^{-1}. \tag{3.4.17}$$

For $z=\epsilon_p(\xi_0)$ we maximize (3.4.17) for $\xi_0\in I_n$ and choose $v=\psi'_m$ in (3.4.16) to obtain

$$\tau^2||\psi'_m||\leq G_n\left(||F_1||_{L^2(Y\setminus R)}+||G_1||_{L^2(Y\setminus R)}+||F_2||_{L^2(R)}+||G_2||_{L^2(R)}\right). \tag{3.4.18}$$

Applying Freidrich's inequality we arrive at the desired upper bound given by

$$\begin{aligned} \tau^2||\psi'_m||_{Y\setminus R} &\leq E_n(||F_1||_{L^2(Y\setminus R)}+||G_1||_{L^2(Y\setminus R)} \\ &\quad +||F_2||_{L^2(R)}+||G_2||_{L^2(R)}), \end{aligned} \tag{3.4.19}$$

where E_n denotes a generic constant depending only on I_n.

The a priori estimate for $\hat{\psi}$ follows from the representation formula (3.2.18) and

$$\|\hat{\psi}\|_{Y\setminus R} \leq H_n, \tag{3.4.20}$$

where the constant H_n depends only on I_n.

Step II. *System of inequalities.*

We apply the a priori estimates developed in Step I to the system of equations (3.2.2), (3.2.15), and solvability conditions (3.2.19) derived in Chapter 3.2. From (3.2.8) and (3.4.19), it follows that

$$\begin{aligned}
&\tau^2||\psi_m'||_{Y\setminus R} \leq \\
&\quad E_n\big[\tau^2(\sum_{l=1}^{m-2}|\xi_l|||\psi_{m-l}||_{Y\setminus R} + \sum_{l=1}^{m-2}|\xi_l|||\psi_{m-1-l}||_{Y\setminus R} \\
&\quad + \sum_{l=1}^{m-2}|\xi_l|||\psi_{m-2-l}||_{Y\setminus R} + ||\psi_{m-1}||_{Y\setminus R} + ||\psi_{m-2}||_{Y\setminus R}) \\
&\quad + \sum_{l=0}^{m-2}|\xi_l|||\psi_{m-2-l}||_{H^1(R)} + \sum_{l=0}^{m-3}|\xi_l|||\psi_{m-3-l}||_{H^1(R)} \\
&\quad + \sum_{l=1}^{m-4}|\xi_l|||\psi_{m-4-l}||_{H^1(R)} + ||\psi_{m-2}||_{H^1(R)} + ||\psi_{m-3}||_{H^1(R)} + ||\psi_{m-4}||_{H^1(R)} \\
&\quad + \sum_{l=0}^{m-2}\sum_{n=0}^{l}|\xi_{m-2-l}||\xi_n|(||\psi_{l-n}||_{Y\setminus R} + ||\psi_{l-n}||_{H^1(R)}) \\
&\quad + \sum_{l=0}^{m-2}|\xi_l|(||\psi_{m-2-1}||_{Y\setminus R} + ||\psi_{m-2-1}||_{H^1(R)})\big].
\end{aligned} \tag{3.4.21}$$

From (3.2.2) and (3.4.10), it follows that

$$\begin{aligned}
&||\tilde{\psi}_m||_{H^1(R)} \leq \\
&\quad B_n\big[\sum_{l=1}^{m-1}\xi_l||\psi_{m-l}||_{H^1(R)} + \sum_{l=0}^{m-1}\xi_l||\psi_{m-1-l}||_{H^1(R)} \\
&\quad + \sum_{l=0}^{m-2}\xi_l||\psi_{m-2-l}||_{H^1(R)} + ||\psi_{m-1}||_{H^1(R)} + ||\psi_{m-2}||_{H^1(R)} \\
&\quad + \sum_{l=1}^{m-1}\sum_{n=0}^{l}\xi_{m-l}\xi_n||\psi_{l-n}||_{H^1(R)} + \sum_{l=1}^{m-1}\xi_l||\psi_{m-l}||_{H^1(R)} + ||\psi_m||_{Y\setminus R}\big]
\end{aligned} \tag{3.4.22}$$

The solvability constant $\mathcal{G}$ in (3.2.19) is bounded away from zero and ∞ for $\xi_0 \in I_n$ Put $m-2 \mapsto m$ in (3.2.19) to obtain the inequality for $|\xi_m|$. The inequality is in terms of a constant C_n depending only on I_n and is given by

$$
\begin{aligned}
|\xi_m| \leq & \\
& C_n\big[\tau^2\big(\sum_{l=0}^{m-1}|\xi_l|||\psi_{m+1-l}||_{Y\setminus R}+\sum_{l=0}^{m-1}|\xi_l|||\psi_{m-l}||_{Y\setminus R} \\
& +2||\psi'_{m+1}||_{Y\setminus R}+||\psi_m||_{Y\setminus R}\big) \\
& +\sum_{l=0}^{m-1}|\xi_l|||\psi_{m-1-l}||_{H^1(R)}+\sum_{l=0}^{m-2}|\xi_l|||\psi_{m-2-l}||_{H^1(R)} \\
& +\sum_{l=1}^{m-1}\sum_{n=0}^{l}|\xi_{m-l}||\xi_n|(||\psi_{l-n}||_{H^1(R)}+||\psi_{l-n}||_{Y\setminus R}) \\
& +2\sum_{l=1}^{m-1}|\xi_l|(||\psi_{m-l}||_{H^1(R)}+||\psi_{m-l}||_{Y\setminus R}) \\
& +(||\tilde{\psi}_m||_{H^1(R)}+||\psi_m||_{Y\setminus R})+(||\tilde{\psi}_m||_{H^1(R)}+||\psi_m||_{Y\setminus R})\big]
\end{aligned}
\tag{3.4.23}
$$

The decompositions (3.2.1), (3.2.7) and bounds (3.4.13), (3.4.20) give

$$
||\psi_m||_{H^1(R)} \leq ||\tilde{\psi}_m||_{H^1(R)}+L_n|\xi_m| \text{ and} \tag{3.4.24}
$$

$$
\|\psi_m\|_{Y\setminus R} \leq \|\psi'_m\|_{Y\setminus R}+H_n|\xi_{m-1}|. \tag{3.4.25}
$$

Here the upper bounds (3.4.21), (3.4.22) (3.4.23), (3.4.24), and (3.4.25) hold for all values of τ for which the branch of the quasistatic dispersion relation ξ_n^0 lies in interval I_n.

Step III. *Majorizing sequence and analyticity of generating functions.*

We simplify the exposition by introducing

$$\overline{p}_m = ||\tau^m \psi_m||_{Y\setminus R} \tag{3.4.26}$$

$$p_m = ||\tau^m \psi_m||_{H^1(R)} \tag{3.4.27}$$

$$\tilde{p}_m = ||\tau^m \tilde{\psi}_m||_{H^1(R)} \tag{3.4.28}$$

$$p'_m = ||\tau^m \psi'_m||_{Y\setminus R} \tag{3.4.29}$$

$$s_m = |\tau^m \xi_m|, \tag{3.4.30}$$

and show that the corresponding series $\sum \rho^m \overline{p}_m$, $\sum \rho^m p_m$, $\sum \rho^m \tilde{p}_m$, $\sum \rho^m p'_m$, and $\sum \rho^m s_m$ converge. This is sufficient to establish summability and convergence for the series (3.3.4) and (3.3.1). Writing (3.4.21), (3.4.22) (3.4.23), (3.4.24), and (3.4.25) in terms of the new notation gives the following system of inequalities. For $m \geq 2$ we have:

$$\begin{aligned} p'_m \leq \\ & E_n\Big[\sum_{l=1}^{m-2} s_l \overline{p}_{m-l} + \tau \sum_{l=0}^{m-2} s_l \overline{p}_{m-1-l} + + \tau^2 \sum_{l=0}^{m-2} s_l \overline{p}_{m-2-l} \\ & + \tau \overline{p}_{m-1} + \tau^2 \overline{p}_{m-2} + \sum_{l=0}^{m-2} s_l p_{m-2-l} + \tau \sum_{l=0}^{m-3} s_l p_{m-3-l} + \tau^2 \sum_{l=0}^{m-4} s_l p_{m-4-l} \\ & + p_{m-2} + \tau p_{m-3} + \tau^2 p_{m-4} + \sum_{l=0}^{m-2} \sum_{n=0}^{l} s_{m-2-l} s_n (\overline{p}_{l-n} + p_{l-n}) \\ & + \sum_{l=0}^{m-2} s_l (\overline{p}_{m-2-l} + p_{m-2-l}) \Big], \end{aligned} \tag{3.4.31}$$

and for $m \geq 1$,

$$\begin{aligned} \tilde{p}_m \leq \\ & B_n\Big[\sum_{l=1}^{m-1} s_l p_{m-l} + \tau \sum_{l=0}^{m-1} s_l p_{m-1-l} + \tau^2 \sum_{l=0}^{m-2} s_l p_{m-2-l} + \tau p_{m-1} + \tau^2 p_{m-2} \\ & + \sum_{l=1}^{m-1} \sum_{n=0}^{l} s_{m-l} s_n p_{l-n} + \sum_{l=1}^{m-1} s_l p_{m-l} + \overline{p}_m \Big]. \end{aligned} \tag{3.4.32}$$

The bounds (3.4.23), (3.4.24), and (3.4.25) yield the following bounds for $m \geq 1$:

$$
\begin{aligned}
s_m \leq & \\
& C_n \big[2\tau p'_{m+1} + \tau \sum_{l=1}^{m-1} s_l \overline{p}_{m+1-l} + \tau^2 \sum_{l=0}^{m-1} s_l \overline{p}_{m-l} \\
& + \tau \sum_{l=0}^{m-1} s_l p_{m-1-l} + \tau^2 \sum_{l=0}^{m-2} s_l p_{m-2-l} + \sum_{l=0}^{m-3} \sum_{n=0}^{l} s_{m-l} s_n (\overline{p}_{l-n} + p_{l-n}) \\
& + 2 \sum_{l=1}^{m} s_l (\overline{p}_{m-l} + p_{m-l}) + 2\tilde{p}_m + (2+\tau^2) \overline{p}_m \big],
\end{aligned} \tag{3.4.33}
$$

$$
p_m \leq \tilde{p}_m + L_n s_m, \tag{3.4.34}
$$

$$
\overline{p}_m \leq p'_m + \tau H_n s_{m-1}. \tag{3.4.35}
$$

The inequalities presented above hold for all τ for which ξ_0^n belongs to I_n. In what follows it is convenient to increase the upper bounds by choosing the maximum value of τ for ξ_0^n in I_n and absorbing this value into the constants B_n, C_n, E_n Additionally any constant factors other than unity that multiply terms in these upper bounds are absorbed into these constants. With these choices the system is written:

$$
\begin{aligned}
p'_m \leq & \\
& E_n \big[\sum_{l=1}^{m-2} s_l \overline{p}_{m-l} + \sum_{l=0}^{m-2} s_l \overline{p}_{m-1-l} + + \sum_{l=0}^{m-2} s_l \overline{p}_{m-2-l} \\
& + \overline{p}_{m-1} + \overline{p}_{m-2} + \sum_{l=0}^{m-2} s_l p_{m-2-l} + \sum_{l=0}^{m-3} s_l p_{m-3-l} + \sum_{l=0}^{m-4} s_l p_{m-4-l} \\
& + p_{m-2} + p_{m-3} + p_{m-4} + \sum_{l=0}^{m-2} \sum_{n=0}^{l} s_{m-2-l} s_n (\overline{p}_{l-n} + p_{l-n}) \\
& + \sum_{l=0}^{m-2} s_l (\overline{p}_{m-2-l} + p_{m-2-l}) \big],
\end{aligned} \tag{3.4.36}
$$

$$\tilde{p}_m \leq \tag{3.4.37}$$
$$B_n\big[\sum_{l=1}^{m-1} s_l p_{m-l} + \sum_{l=0}^{m-1} s_l p_{m-1-l} + \sum_{l=0}^{m-2} s_l p_{m-2-l} + p_{m-1} + p_{m-2}$$
$$+ \sum_{l=1}^{m-1}\sum_{n=0}^{l} s_{m-l}s_n p_{l-n} + \sum_{l=1}^{m-1} s_l p_{m-l} + \overline{p}_m\big],$$

$$s_m \leq \tag{3.4.38}$$
$$C_n\big[p'_{m+1} + \sum_{l=1}^{m-1} s_l \overline{p}_{m+1-l} + \sum_{l=0}^{m-1} s_l \overline{p}_{m-l}$$
$$+ \sum_{l=0}^{m-1} s_l p_{m-1-l} + \sum_{l=0}^{m-2} s_l p_{m-2-l} + \sum_{l=0}^{m-3}\sum_{n=0}^{l} s_{m-l}s_n(\overline{p}_{l-n} + p_{l-n})$$
$$+ \sum_{l=1}^{m} s_l(\overline{p}_{m-l} + p_{m-l}) + \tilde{p}_m + \overline{p}_m\big],$$

$$p_m \leq C_4(\tilde{p}_m + s_m), \tag{3.4.39}$$

$$\overline{p}_m \leq C_5(p'_m + s_{m-1}), \tag{3.4.40}$$

where C_4, C_5 are positive constants depending only on I_n and $m \geq 1$.

We now introduce a majorizing sequence $\{(a_m, b_m, c_m, d_m, e_m)\}_{m=0}^{\infty}$ for which

$$\begin{aligned}
\sum_{n=0}^{\infty} a_n\rho^n = &\quad \rho a(\rho) + \overline{p}_0 &&\geq \sum_{n=0}^{\infty} \overline{p}_n\rho^n \\
\sum_{n=1}^{\infty} b_n\rho^n = &\quad b(\rho) &&\geq \sum_{n=1}^{\infty} \tilde{p}_n\rho^n \\
\sum_{n=0}^{\infty} c_n\rho^n = &\quad c(\rho) &&\geq \sum_{n=0}^{\infty} s_n\rho^n \\
\sum_{n=0}^{\infty} d_n\rho^n = &\quad d(\rho) &&\geq \sum_{n=0}^{\infty} p_n\rho^n \\
\sum_{n=2}^{\infty} e_n\rho^n = &\quad \rho e(\rho) &&\geq \sum_{n=2}^{\infty} p'_n\rho^n,
\end{aligned} \tag{3.4.41}$$

to show that the generating functions $a(\rho), \ldots, e(\rho)$ are analytic in a neighborhood of the origin $\rho = 0$.

The majorizing sequence is chosen so that the system of inequalities (3.4.36), (3.4.37), (3.4.38), (3.4.39), (3.4.40) hold with equality for $a_m = \overline{p}_m$, $b_m = \tilde{p}_m$, $c_m = s_m, p_m = d_m$, and $e_m = p'_m$. Indeed, for this choice one observes that $\overline{p}_m \leq a_m$, $\tilde{p}_m \leq b_m$, $s_m \leq c_m$, $p_m \leq d_m$, and $p'_m \leq e_n$. Enforcing equality in (3.4.36), (3.4.37), (3.4.38), (3.4.39), (3.4.40), multiplying each by the appropriate power of ρ and summation delivers the equivalent system for the generating functions $a(\rho), b(\rho), c(\rho), d(\rho), e(\rho)$ given by:

$$A_i(a, b, c, d, e, \rho) = 0, \ i = 1, \dots 5, \tag{3.4.42}$$

where:

$$A_1(a, b, c, d, e, \rho) = \tag{3.4.43}$$
$$\overline{p}_1 - a + C_5(e + (c - s_0)),$$

$$A_2(a, b, c, d, e, \rho) = \tag{3.4.44}$$
$$\begin{aligned} &- b + B_n\big[(c - s_0)(d - p_0) + (cd + d)(\rho + \rho^2) \\ &+ c^2 d - s_0^2 p_0 - \rho s_0 s_1 (p_0 + p_1) \\ &- s_0 p_0 (c - s_0) - s_0 cd + s_0(\rho(s_0 p_1 + s_1 p_0) + s_0 p_0) \\ &+ (c - s_0)(d - p_0) + \rho a\big] \end{aligned}$$

$$A_3(a, b, c, d, e, \rho) = \tag{3.4.45}$$
$$\begin{aligned} &-(c - s_0) + C_n\big[(a - \overline{p}_1)(c - s_0) + e + \rho ac + \rho(a + cd) \\ &+\rho^2 cd + c^2(\rho a + \overline{p}_0) - s_0 \overline{p}_0 c - s_0((\rho a + \overline{p}_0)c - s_0 \overline{p}_0) \\ &+(c - s_0)(d - p_0) + b - \rho(\rho a + \overline{p}_0) c s_1 \\ &-\rho^2 s_2(\rho a + \overline{p}_0)c + c^2 d \\ &-s_0 p_0 c - s_0(cd - s_0 p_0) - \rho cd(s_1 + \rho s_2)\big] \end{aligned}$$

$$A_4(a, b, c, d, e, \rho) = (d - p_0) + C_4(b + (c - s_0)). \tag{3.4.46}$$

$$A_5(a,b,c,d,e,\rho) = \tag{3.4.47}$$
$$-e + E_n\big[(a-\overline{p}_1)(c-s_0) + \rho ac + \rho(\rho a + \overline{p}_0)c + \rho a$$
$$+\rho(\rho a + \overline{p}_0)) + (c+1)d(\rho + \rho^2 + \rho^3)$$
$$+\rho c(c+1)(\rho a + \overline{p}_0 + d)\}\big]$$

One can check A_1, A_2, A_3, A_4 and A_5 vanish for $a = \overline{p}_1 = \|\psi_1\|_{Y\setminus R}$, $b = 0$, $c = s_0 = |\xi_0^n|$, $d = p_0 = \|\psi_0\|_{H^1(R)}$, $e = 0$, and $\rho = 0$. Moreover, the determinant of the Jacobian matrix with respect to the first five variables at this point, i.e., $(a,b,c,d,e,\rho) = (\overline{p}_1, 0, s_0, p_0, 0, 0)$, is

$$det\frac{\partial(A_1,A_2,A_3,A_4,A_5)}{\partial(a,b,c,d,e)}(\overline{p}_1,0,s_0,p_0,0,0) = 1. \tag{3.4.48}$$

Thus the implicit function theorem for functions of several complex variables guarantees that the generating functions a, b, c, d, e are analytic within a neighborhood of $\rho = 0$ and we conclude that the series on the right hand side of the inequalities (3.4.41) are convergent. Here $\overline{p}_0 = \|\psi_0\|_{Y\setminus R} = |Y \setminus R|^{1/2}$ and the initial data p_0, $\overline{p}_1$ are bounded functions of ξ_0^n on I_n. Choosing the maximum values of p_0, $\overline{p}_1$, ξ_0^n, as ξ_0^n varies over I_n delivers a majorizing sequence with radius of convergence R depending only on I_n. It now follows that the series (3.3.1) converges and that (3.3.4) is summable for $0 \le \rho < R$.

3.5 Power series solution of cell problem

In this part we show that the functions defined by the power series solve (2.1.4). For ξ_0^n in I_n recall the series (2.1.5), (2.1.6)

$$u = \sum_{m=0}^{\infty} \eta^m u_m \tag{3.5.1}$$
$$\xi = \sum_{m=0}^{\infty} \eta^m \xi_m \tag{3.5.2}$$

with $u_m = i^m \underline{u}_0 \psi_m$ and $\eta = \rho\tau$ converges for $0 < \rho < R$. For $v \in H^1_{per}(Y)$ and $0 \leq \rho < R$. We define

$$\begin{aligned} a^\eta(v) := \quad & \int_H \tau^2(\xi - \epsilon_r \frac{\omega_p^2}{c^2})(\nabla_y + i\eta\hat{\kappa})u \cdot \overline{(\nabla_y + i\eta\hat{\kappa})v} \\ & + \int_P \tau^2 \xi (\nabla_y + i\eta\hat{\kappa})u \cdot \overline{(\nabla_y + i\eta\hat{\kappa})v} \\ & + \int_R \eta^2(\xi - \epsilon_r \frac{\omega_p^2}{c^2})(\nabla_y + i\eta\hat{\kappa})u \cdot \overline{(\nabla_y + i\eta\hat{\kappa})v} \\ & - \int_Y \eta^2 \xi (\xi - \epsilon_r \frac{\omega_p^2}{c^2}) u\overline{v}. \end{aligned} \tag{3.5.3}$$

First observe that $a^\eta(v)$ has a convergent power series in η that is obtained by inserting u and ξ into the above expression and expanding in powers of η . The coefficients of this expansion are exactly the left-hand side of equation (2.1.8). Since ψ_m satisfies (2.1.8), all coefficients of the power series expansion of $a^\eta(v)$ are zero and we conclude that $a^\eta(v) = 0$ for all $v \in H^1_{per}(Y)$, $0 \leq \rho < R$. Thus we conclude that the pair (u, ξ) satisfies (2.1.4).

Next we record the following property of the sequence $\{\xi_m\}$ that follows directly from the variational formulation of the problem and the power series solution.

Theorem 3.5.1. *The functions ξ_m are real for all m.*

Proof. Setting $v = u$ in (2.1.4) delivers a quadratic equation for ξ. Since the discriminant greater than zero, we conclude that ξ is real and it follows that ξ_m, $m = 1, \ldots,$ are real. □

With these results in hand, Theorems 3.3.1 and 3.3.2 now follow from the convergence established in Chapter 3.4 together with Theorem 3.2.1.

3.6 Application of the power series representation to homogenization in metamaterials

The power series representation is used to show that branches of solutions (3.1.13) corresponding to $\mu_{eff}(\xi_0) < 0$, $\epsilon_{eff}^{-1}(\xi_0)\hat{\kappa}\cdot\hat{\kappa} < 0$ correspond to frequency intervals where the phase velocity in the effective medium is opposite to the direction of energy flow. For H-polarized Bloch waves, the magnetic field $\mathbf{H}(\mathbf{x}/d) = (0, 0, H_3(\mathbf{x}/d))$ where $H_3(\mathbf{x}/d)$ is given by (3.3.3) and the electric field $\mathbf{E}(\mathbf{x}/d) = (E_1(\mathbf{x}/d), E_2(\mathbf{x}/d), 0)$. Both fields are related through (1.2.3). Therefore

$$\mathbf{E}(\mathbf{x}/d) = \frac{ic}{\omega a_d}\partial_{x_2}H_3(\mathbf{x}/d)\mathbf{e_1} - \frac{ic}{\omega a_d}\partial_{x_1}H_3(\mathbf{x}/d)\mathbf{e_2}, \tag{3.6.1}$$

where $\mathbf{e_i}$ is the unit vector along the x_i direction for $i = 1, 2, 3$. The time average of the Poynting vector is given by

$$\begin{aligned}\mathbf{P}^d &= \frac{1}{2}Re[\mathbf{E}(\mathbf{x}/d)\times\overline{\mathbf{H}(\mathbf{x}/d)}] \\ &= \frac{1}{2}Re[E_2(\mathbf{x}/d)\overline{H_3(\mathbf{x}/d)}\mathbf{e_1} - E_1(\mathbf{x}/d)\overline{H_3(\mathbf{x}/d)}\mathbf{e_2}].\end{aligned} \tag{3.6.2}$$

Consider any fixed averaging domain D transverse to the cylinders and the spatial average of the electromagnetic energy flow along the direction $\hat{\kappa}$ over this domain is written $\langle\mathbf{P}\cdot\hat{\kappa}\rangle_D$. Substituting (3.3.3) and (3.6.1) into (3.6.2) and taking the limit of (3.6.2) as $d \to 0$ shows that the average electromagnetic energy flow along the direction $\hat{\kappa}$ is given by

$$\langle\mathbf{P}\cdot\hat{\kappa}\rangle_D = \frac{1}{2}|\underline{u_0}|^2 n_{eff}\epsilon_{eff}^{-1}\hat{\kappa}\cdot\hat{\kappa}. \tag{3.6.3}$$

In the $d \to 0$ limit, the phase velocity is along the direction $\hat{\kappa}$ and determined by

$$\mathbf{v}_p = \frac{c}{n_{eff}}\hat{\kappa}. \tag{3.6.4}$$

Recall that we have pass bands over frequency intervals where $\epsilon_{eff}^{-1}\hat{\kappa}\cdot\hat{\kappa}$ and μ_{eff} are of the same sign. With this in mind equations (3.6.3) and (3.6.4) show that

in the homogenization limit the energy flow and phase velocity are in opposite directions over frequency intervals where the double negative property happens, i.e., $\epsilon_{eff}^{-1}\hat{\kappa}\cdot\hat{\kappa} < 0$ and $\mu_{eff} < 0$. These results are indicative of negative index behavior in the homogenization limit.

These results extend the methods of homogenization theory to identify frequency intervals characterized by negative index behavior. Earlier work delivers formulas for frequency-dependent effective magnetic permeability together with conditions for generation of negative effective permeability [8], [9], [10], [13], [15] and [26]. For periodic arrays made from metal fibers a homogenization theory delivering negative effective dielectric constant [7] has been established. A novel method for creating metamaterials with prescribed effective dielectric permittivity and effective magnetic permeability at a fixed frequency is developed in [30].

Chapter 4
Simulation

In this chapter we choose metamaterials made from subwavelength periodic arrangements of nonmagnetic infinitely long circular coated rods with plasmonic coating with dielectric constant $\epsilon_P(\omega) = 1 - \frac{\omega_p^2}{\omega^2}$ and core material with frequency independent dielectric constant $\epsilon_R = \epsilon_r/d^2$ (Figure 4.1). Although our microgeom-

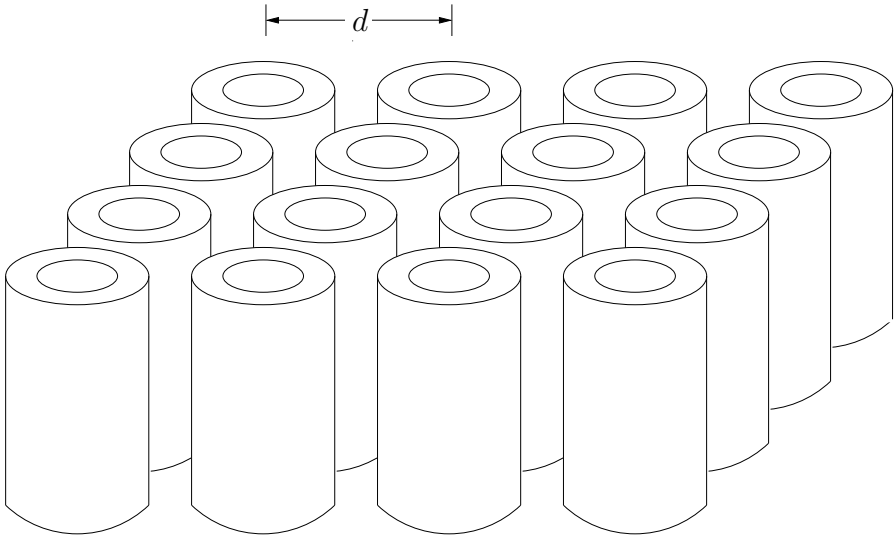

FIGURE 4.1: Periodic arrangements of circular coated cylinders with period d

etry is different from the one we consider in Chapter 2 and Chapter 3, a straightforward analysis shows that all the results discussed in the previous two chapters are also true for the coated cylinder microgeometry.

4.1 Generalized electrostatic resonances for circular coated cylinders and the Rayleigh identity

In this part we develop a Rayleigh's identity for the eigenfunctions associated with generalized electrostatic resonances for coated circular cylinders. The Rayleigh

method [45] has been generalized and applied to the analysis of wave propagation and the effective transport properties of composites and the approach taken here is motivated by the recent work [29], [32] and [37]. The electrostatic resonances λ_h in (3.1.12) are found by solving the following problem for the potential u inside a unit cell, i.e., $d = 1$:

$$\begin{cases} \Delta u = 0 \quad \text{in } H, \\ \Delta u = 0 \quad \text{in } P, \end{cases} \tag{4.1.1}$$

with the boundary conditions

$$\begin{cases} u|^- = u|^+ \quad \text{on } \partial P, \\ \partial_r u|_{r=a} = 0 \quad \text{on } \partial R, \\ \lambda[\partial_r u]^-_+ = -\frac{1}{2}(\partial_r u^- + \partial_r u^+) \text{ on } \partial P, \\ u \text{ is } Y\text{-periodic .} \end{cases} \tag{4.1.2}$$

Consequently, in polar coordinates (r, θ) , the expansions of the potential $u(r, \theta)$ are

$$u_p(r, \theta) = \sum_{l=1}^{\infty} (A_l r^l + B_l r^{-l}) \cos l\theta \qquad \text{in } P, \tag{4.1.3}$$

$$u_h(r, \theta) = \sum_{l=1}^{\infty} (C_l r^l + D_l r^{-l}) \cos l\theta \qquad \text{in } H. \tag{4.1.4}$$

From the boundary conditions (4.1.2), we can express A_l, C_l and D_l in terms of B_l. Therefore we get

$$\begin{cases} A_l = a^{-2l} B_l, \\ C_l = \left(\frac{a^{2l} b^{-2l} - 2\lambda}{1 - 2\lambda}\right) a^{-2l} B_l, \\ D_l = \left(\frac{a^{-2l} b^{2l} - 2\lambda}{1 - 2\lambda}\right) B_l. \end{cases} \tag{4.1.5}$$

The surface charge density $Q_s(\theta)$ is defined by

$$\begin{aligned} Q_s(\theta) &= (\partial_r u_p - \partial_r u_h)|_{r=b} \\ &= 2\sum_{l=1}^{\infty} \big(\frac{b^{l-1}a^{-2l} - b^{-(l+1)}}{1-2\lambda}\big) l B_l \cos l\theta. \end{aligned} \tag{4.1.6}$$

The potential at an arbitary point $G(r,\theta)$ is given by

$$u(r,\theta) = -\frac{1}{2\pi}\sum_j \int_{\partial s_j} Q^j_{s_j}(\mathbf{t_{(s_j)}}) \ln(|\mathbf{r} - \mathbf{t_{(s_j)}}|)\mathbf{ds_j}. \tag{4.1.7}$$

In the summation j refers to the jth cylinder and the vector $\mathbf{t_{(s_j)}}$ extended from the origin to the area element ds_j on its shell. $Q^j_{s_j}(\mathbf{t_{(s_j)}})$ is the surface charge density at this area element. We sum over all cylinders in the lattice and integrate over the entire surface of each cylinder. We introduce the vectors $\boldsymbol{\rho_j}$ pointing from the center of the jth cylinder to the point G and $\mathbf{s}$ pointing from the center of the jth cylinder to ∂s_j .

From Figure 4.2 , it is easy to see that

$$\mathbf{r} - \mathbf{t_{(s_j)}} = \boldsymbol{\rho_j} - \mathbf{s}. \tag{4.1.8}$$

First suppose that the field point G is in the shell of the central cylinder ,i.e., $a < r < b$. Since $|\mathbf{s}| = \mathbf{b}, \rho_\mathbf{0} = \mathbf{r}$ and $|\boldsymbol{\rho_j}| > b \ \ \forall j \neq 0, \ a < |\mathbf{r}| < \mathbf{b}$ for $\mathbf{j = 0}$. Then we can expand the logarithms in (4.1.7)

$$\begin{aligned} \ln|\mathbf{r} - \mathbf{t_{(s_j)}}| &= \ln|\boldsymbol{\rho_j} - \mathbf{s}| \\ &= \begin{cases} \ln\rho_j - \sum_{n=1}^{\infty} \frac{1}{n}(\frac{b}{\rho_i})^n \cos n(\theta' - \theta_j) & j \neq 0, \\ \ln b - \sum_{n=1}^{\infty} \frac{1}{n}(\frac{r}{b})^n \cos n(\theta' - \theta) & j = 0, \end{cases} \end{aligned} \tag{4.1.9}$$

where θ' is the polar angle defining the orientation of $\mathbf{s}$ and θ_j specifies the direction of $\boldsymbol{\rho_j}$. For the jth cylinder the surface charge density takes the form (4.1.6) depending on θ'. From (4.1.7), (4.1.9) and the orthonormality properties of Sines

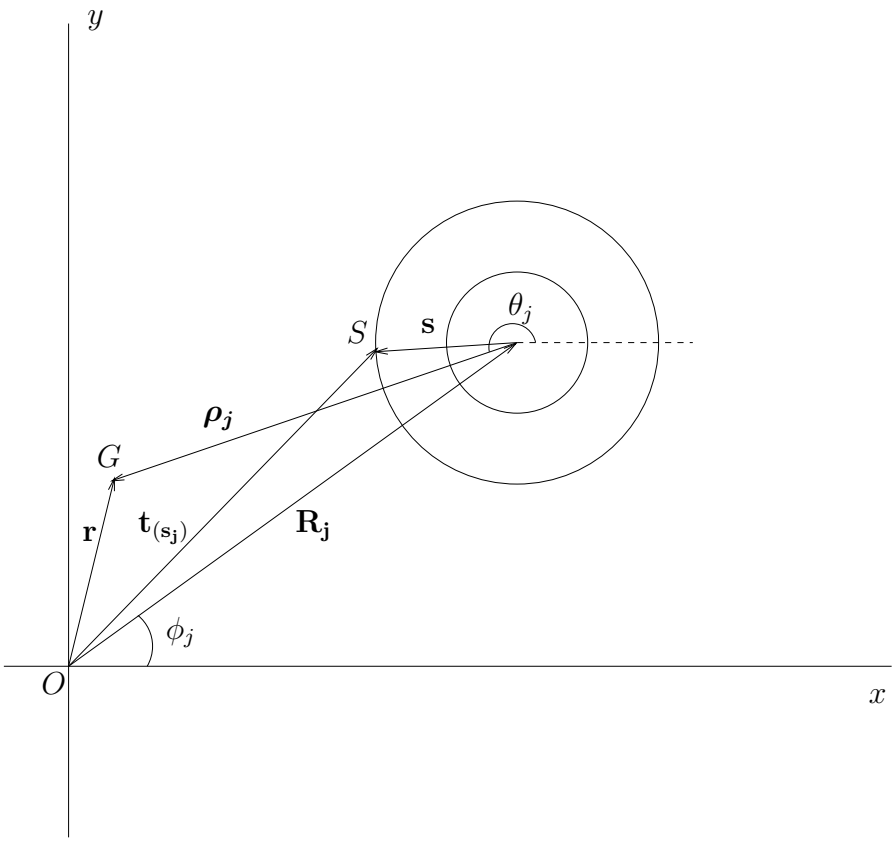

FIGURE 4.2: G is a typical field point while S present a point on the shell boundary of the jth cylinder.

and Cosines, we find

$$\begin{aligned} u(r,\theta) &= \sum_{l=1}^{\infty} \frac{1}{1-2\lambda}(a^{-2l}-b^{-2l})B_l r^l \cos l\theta \\ &\quad + \sum_{j\neq 0}\sum_{l=1}^{\infty} \frac{1}{1-2\lambda}\Big(\frac{a^{-2l}b^{2l}-1}{\rho_j^l}\Big)B_l \cos l\theta_j \end{aligned} \tag{4.1.10}$$

for $a < r < b$.

In (4.1.10) the first sum is from the central cylinder and the second sum is over all the other cylinders. In the shell , we must have

$$u(r,\theta) = u_p(r,\theta) = \sum_{l=1}^{\infty}(A_l r^l + B_l r^{-l})\cos l\theta. \tag{4.1.11}$$

Plugging (4.1.5) and (4.1.10) into (4.1.11) , we obtain the Rayleigh's identity for a square array of coated cylinders:

$$\sum_{l=1}^{\infty}\left[\left(\frac{b^{-2l}-2\lambda a^{-2l}}{1-2\lambda}\right)r^{l}+r^{-l}\right]B_l\cos l\theta$$
$$=\sum_{j\neq 0}\sum_{l=1}^{\infty}\left(\frac{a^{-2l}b^{2l}-1}{1-2\lambda}\right)\frac{B_l}{\rho_j^{l}}\cos l\theta_j \qquad (4.1.12)$$

for $a<r<b$.

Next we suppose that the field point G is outside the shell of the the central cylinder, i.e., $r>b$. The proof is similar to the case in the shell P. Since $r>b$, (4.1.9) changes to be

$$\begin{aligned}\ln|\mathbf{r}-\mathbf{t}_{(\mathbf{s_j})}| &= \ln|\boldsymbol{\rho_j}-\mathbf{s}|\\ &= \begin{cases}\ln\rho_j-\sum_{n=1}^{\infty}\frac{1}{n}(\frac{b}{\rho_i})^n\cos n(\theta'-\theta_j) & j\neq 0,\\ \ln r-\sum_{n=1}^{\infty}\frac{1}{n}(\frac{b}{r})^n\cos n(\theta'-\theta) & j=0.\end{cases}\end{aligned} \qquad (4.1.13)$$

Then like (4.1.10) , we have

$$\begin{aligned}u(r,\theta) &= \sum_{l=1}^{\infty}\frac{1}{1-2\lambda}(a^{-2l}b^{2l}-1)B_l r^{-l}\cos l\theta\\ &\quad+\sum_{j\neq 0}\sum_{l=1}^{\infty}\frac{1}{1-2\lambda}\big(\frac{a^{-2l}b^{2l}-1}{\rho_j^{l}}\big)B_l\cos l\theta_j \qquad (4.1.14)\end{aligned}$$

for $r>b$. In the host H, we must have

$$u(r,\theta)=u_h(r,\theta)=\sum_{l=1}^{\infty}(C_l r^{l}+D_l r^{-l})\cos l\theta. \qquad (4.1.15)$$

A calculation similar to the previous in the shell shows that (4.1.12) holds for $r>b$. Therefore (4.1.12) is true for all $r>a$.

4.2 Numerical calculation of generalized electrostatic spectra for coated cylinders

In this part we numerically calculate the generalized electrostatic spectra for coated cylinders. We set $r=b$ in (4.1.12) and apply Rayleigh's method [45] to recover a

linear system of equations to determine λ and $\{B_l\}_{l=1}^{\infty}$. Let R_j be the distance from the origin to the center of the jth cylinder and the ϕ_j be the polar angle defining the orientation of $\mathbf{R_j}$ (See Figure 4.2). Then for $r = b$ we have

$$\rho_j \cos\theta_j + i\rho_j \sin\theta_j = (b\cos\theta + ib\sin\theta) - (R_j \cos\phi_j + iR_j \sin\phi_j) \tag{4.2.1}$$

The Rayleigh's identity (4.1.12) with $r = b$ becomes

$$\begin{aligned}
&Re\sum_{l=1}^{\infty}\left[\left(\frac{b^{-2l} - 2\lambda a^{-2l}}{1-2\lambda}\right) B_l(b\cos\theta + ib\sin\theta)^l + B_l(b\cos\theta + ib\sin\theta)^{-l}\right] \\
&= Re\sum_{j\neq 0}[\left(\frac{a^{-2}b^2 - 1}{1-2\lambda}\right) B_1\left((b\cos\theta + ib\sin\theta) - (R_j\cos\phi_j + iR_j\sin\phi_j)\right)^{-1} \\
&+ \left(\frac{a^{-4}b^4 - 1}{1-2\lambda}\right) B_2\left((b\cos\theta + ib\sin\theta) - (R_j\cos\phi_j + iR_j\sin\phi_j)\right)^{-2} \\
&+ \left(\frac{a^{-8}b^8 - 1}{1-2\lambda}\right) B_3\left((b\cos\theta + ib\sin\theta) - (R_j\cos\phi_j + iR_j\sin\phi_j)\right)^{-3} \\
&+ \cdots]
\end{aligned} \tag{4.2.2}$$

Using the generalized binomial theorem on the right-hand side of (4.2.2), we have

$$\begin{aligned}
&Re\sum_{l=1}^{\infty}\left[\left(\frac{b^{-2l} - 2\lambda a^{-2l}}{1-2\lambda}\right) B_l(b\cos\theta + ib\sin\theta)^l + B_l(b\cos\theta + ib\sin\theta)^{-l}\right] \\
&= Re\sum_{j\neq 0}[\left(\frac{a^{-2}b^2 - 1}{1-2\lambda}\right) B_1(-1)^1(R_j\cos\phi_j + iR_j\sin\phi_j)^{-1} \\
&\sum_{k=0}^{\infty}\left(\frac{b\cos\theta + ib\sin\theta}{R_j\cos\phi_j + iR_j\sin\phi_j}\right)^k \\
&+ \left(\frac{a^{-4}b^4 - 1}{1-2\lambda}\right) B_2(-1)^2(R_j\cos\phi_j + iR_j\sin\phi_j)^{-2} \\
&\sum_{k=0}^{\infty}\binom{2+k-1}{k}\left(\frac{b\cos\theta + ib\sin\theta}{R_j\cos\phi_j + iR_j\sin\phi_j}\right)^k \\
&+ \left(\frac{a^{-8}b^8 - 1}{1-2\lambda}\right) B_3(-1)^3(R_j\cos\phi_j + iR_j\sin\phi_j)^{-3} \\
&\sum_{k=0}^{\infty}\binom{3+k-1}{k}\left(\frac{b\cos\theta + ib\sin\theta}{R_j\cos\phi_j + iR_j\sin\phi_j}\right)^k \\
&+ \cdots].
\end{aligned} \tag{4.2.3}$$

Equating the coefficients of $\cos l\theta$ in (4.2.3) between left- and right-hand sides, we obtain

$$\begin{aligned}
&\left(\frac{b^{-2l}-2\lambda a^{-2l}}{1-2\lambda}\right)B_l b^l + B_l b^{-l} \\
&= Re\{\sum_{j\neq 0}[\left(\frac{a^{-2}b^2-1}{1-2\lambda}\right)B_1(-1)^1(R_j\cos\phi_j + iR_j\sin\phi_j)^{-l-1}b^l \\
&\quad + \left(\frac{a^{-4}b^4-1}{1-2\lambda}\right)B_2(-1)^2(R_j\cos\phi_j + iR_j\sin\phi_j)^{-l-2}\binom{2+l-1}{l}b^l \\
&\quad + \left(\frac{a^{-8}b^8-1}{1-2\lambda}\right)B_3(-1)^3(R_j\cos\phi_j + iR_j\sin\phi_j)^{-l-3}\binom{3+l-1}{l}b^l \\
&\quad + \cdots]\} \\
&= \sum_{j\neq 0}\sum_{m=1}^{\infty}\left[\left(\frac{a^{-2m}b^{2m}-1}{1-2\lambda}\right)\binom{m+l-1}{l}B_m(-1)^m\frac{\cos(l+m)\phi_j}{R_j^{l+m}}b^l\right] \\
&= \sum_{m=1}^{\infty}\left[\left(\frac{a^{-2m}b^{2m}-1}{1-2\lambda}\right)\binom{m+l-1}{l}B_m(-1)^m S_{l+m}b^l\right], \qquad (4.2.4)
\end{aligned}$$

where the quantities S_n are the lattice sums

$$S_n = \sum_{j\neq 0}\frac{\cos n\phi_j}{R_j^n}. \qquad (4.2.5)$$

A list of numerical values for S_n is tabulated in the paper of Perrins Perrins et. al. [37]. Rewriting (4.2.4) as

$$\begin{aligned}
\lambda B_l &= \left(\frac{b^{-2l}}{a^{-2l}+b^{-2l}}\right)B_l \\
&\quad -\frac{1}{2(a^{-2l}+b^{-2l})}\sum_{m=1}^{\infty}(a^{-2m}b^{2m}-1)\binom{m+l-1}{l}(-1)^m S_{l+m}B_m. \qquad (4.2.6)
\end{aligned}$$

The system (4.2.6) may be written in the matrix form

$$AB = \lambda B, \qquad (4.2.7)$$

where $B = (B_1, B_2, B_3, \cdots)^T$ and the infinite dimentional matrix A has the elements

$$A_{lm} = \begin{cases} \frac{b^{-2l}}{a^{-2l}+b^{-2l}} - \frac{1}{2(a^{-2l}+b^{-2l})}(a^{-2m}b^{2m}-1)\binom{m+l-1}{l}(-1)^m S_{l+m} & l = m, \\ -\frac{1}{2(a^{-2l}+b^{-2l})}(a^{-2m}b^{2m}-1)\binom{m+l-1}{l}(-1)^m S_{l+m} & l \neq m. \end{cases} \qquad (4.2.8)$$

We solve (4.2.7) numerically, truncating the sum after N terms to find the approximation of the potential u and the generalized electrostatic resonances. Table 4.1 gives the eigenvalues corresponding to different N for $a = 0.2$ and $b = 0.4$. These numerical results confirm that the eigenvalues have an accumulation point at 0. For illustration, if λ is the first eigenvalue 3.5080×10^{-1} with $a = 0.2$ and $b = 0.4$, then we notice that $B_1 \approx 1$ and the remaining coefficients B_l's are close to 0. Hence (4.1.10) and (4.1.14) show that the potential $u(r, \theta)$ is well approximated by

TABLE 4.1: The eigenvalues corresponding to $N = 10, 15, 20$ with $a = 0.2$, $b = 0.4$.

	$N = 10$	$N = 15$	$N = 20$
λ	3.5080×10^{-1}	3.5080×10^{-1}	3.5080×10^{-1}
	1.5379×10^{-2}	1.5379×10^{-2}	1.5379×10^{-2}
	9.7557×10^{-4}	9.7557×10^{-4}	9.7557×10^{-4}
	6.1031×10^{-5}	6.1031×10^{-5}	6.1031×10^{-5}
	3.8147×10^{-6}	3.8147×10^{-6}	3.8147×10^{-6}
	-2.0285×10^{-3}	2.3842×10^{-7}	2.3842×10^{-7}
	-5.5339×10^{-3}	1.4901×10^{-8}	1.4901×10^{-8}
	-1.5014×10^{-2}	9.3132×10^{-10}	9.3132×10^{-10}
	-4.4538×10^{-2}	-2.8905×10^{-10}	5.8208×10^{-10}
	-4.7947×10^{-2}	-7.6128×10^{-10}	3.6380×10^{-10}
		-2.0285×10^{-3}	-1.6665×10^{-5}
		-5.5339×10^{-3}	-4.2856×10^{-5}
		-1.5014×10^{-2}	-1.1088×10^{-4}
		-4.4538×10^{-2}	-2.8905×10^{-4}
		-4.7947×10^{-2}	-7.6128×10^{-4}
			-2.0285×10^{-3}
			-5.5339×10^{-3}
			-1.5014×10^{-2}
			-4.4538×10^{-2}
			-4.7947×10^{-2}

$$u(r,\theta) \approx \begin{cases} \frac{1}{1-2\lambda}(a^{-2}-b^{-2})r\cos\theta + \sum_{j\neq 0}\frac{1}{1-2\lambda}\left(\frac{a^{-2}b^2-1}{\rho_j}\right)\cos\theta_j & \text{in } P, \\ \frac{1}{1-2\lambda}(a^{-2}b^2-1)r^{-1}\cos\theta + \sum_{j\neq 0}\frac{1}{1-2\lambda}\left(\frac{a^{-2}b^2-1}{\rho_j}\right)\cos\theta_j & \text{in } H. \end{cases} \tag{4.2.9}$$

Equivalently (4.1.3) and (4.1.4) show

$$u(r,\theta) \approx \begin{cases} a^{-2} r\cos\theta + r^{-1}\cos\theta & \text{in } P, \\ \left(\frac{a^2 b^{-2} - 2\lambda}{1-2\lambda}\right) a^{-2} r\cos\theta + \left(\frac{a^{-2} b^2 - 2\lambda}{1-2\lambda}\right) r^{-1}\cos\theta & \text{in } H. \end{cases} \tag{4.2.10}$$

The the solution u corresponding to the first two eigenvalues with $a = 0.2$ and $b = 0.4$ are illustrated in Figure 4.3.

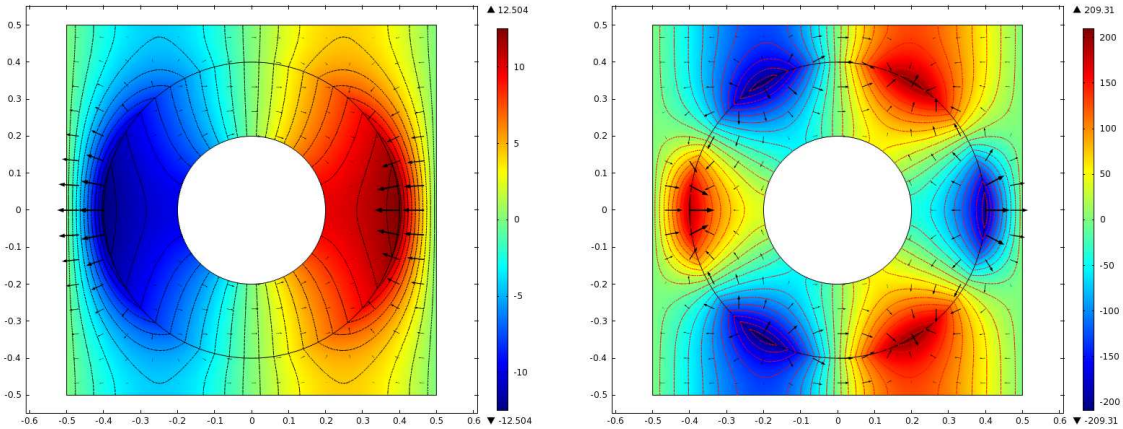

(a) (b)

FIGURE 4.3: (a) the solution corresponding to the eigenvalue $\lambda = 3.5080 \times 10^{-1}$; (b) the solution corresponding to the eigenvalue $\lambda = 1.5379 \times 10^{-2}$.

4.3 Numerical calculation of the dispersion relation and comparison with power series

In this part we verify that the leading order dispersion relation expressed in terms of effective properties is a good predictor of the dispersive behavior of the metamaterial for periods with finite size $d > 0$. The usefulness of the effective properties for predicting metamaterial behavior away from the homogenization limit can be explicitly seen from power series formula for the dispersion relation. To proceed we fix $d = c/\omega_p$ and the dimensionless ratio $\rho = d/\sqrt{\epsilon_r}$. With this choice of variables the frequency dependent effective magnetic permeability μ_{eff} and effective

dielectric permittivity ϵ_{eff} are written as

$$\mu_{eff}(\omega_0/\omega_p) = \int_Y \psi_0 = \theta_H + \theta_P + \sum_{n=1}^{\infty} \frac{\mu_n < \phi_n >_R^2}{\rho^{-2}\left(\mu_n\rho^2 - (\frac{\omega_0}{\omega_p})^2\right)} \tag{4.3.1}$$

and

$$\epsilon_{eff}^{-1}(\omega_0/\omega_p)\hat{\kappa}\cdot\hat{\kappa} = \theta_H + \frac{(\frac{\omega_0}{\omega_p})^2}{(\frac{\omega_0}{\omega_p})^2 - 1}\theta_P \tag{4.3.2}$$
$$- \sum_{-\frac{1}{2}<\lambda_h<\frac{1}{2}} \left(\frac{\left((\frac{\omega_0}{\omega_p})^2 - 1\right)^2 |\alpha_{\lambda_h}^{(1)}|^2 + 2\left((\frac{\omega_0}{\omega_p})^2 - 1\right)\alpha_{\lambda_h}^{(1)}\alpha_{\lambda_h}^{(2)} + |\alpha_{\lambda_h}^{(2)}|^2}{\left((\frac{\omega_0}{\omega_p})^2 - (\lambda_h + \frac{1}{2})\right)\left((\frac{\omega_0}{\omega_p})^2 - 1\right)} \right).$$

In these variables the leading order dispersion relation is given by

$$(dk)^2 = (\frac{\omega_0}{\omega_p})^2 n_{eff}^2, \tag{4.3.3}$$

where the effective index of diffraction n_{eff}^2 depends upon the direction of propagation $\hat{\kappa}$ and normalized frequency $\frac{\omega_0}{\omega_p}$ and is written

$$n_{eff}^2 = \mu_{eff}(\frac{\omega_0}{\omega_p})/(\epsilon_{eff}^{-1}(\frac{\omega_0}{\omega_p})\hat{\kappa}\cdot\hat{\kappa}). \tag{4.3.4}$$

The dispersion relation for the metamaterial crystal in the new variables is given by

$$\left(\frac{\omega}{\omega_p}\right)^2 = \left(\frac{\omega_0}{\omega_p}\right)^2 + \sum_{l=1}^{\infty}(dk)^l \left(\frac{\omega_l}{\omega_p}\right)^2, \tag{4.3.5}$$

for

$$\{-2\pi \le dk\hat{\kappa}_1 \le 2\pi, -2\pi \le dk\hat{\kappa}_2 \le 2\pi\}. \tag{4.3.6}$$

It is clear from (4.3.5) that the roots $\frac{\omega_0}{\omega_p}$ of the effective dispersion relation (4.3.3) determines the leading order dispersive behavior for periods of finite size. We point out that the notion of effective properties for metamaterials has proved to be an elegant concept for explaining experimental results. Here it is seen that the power

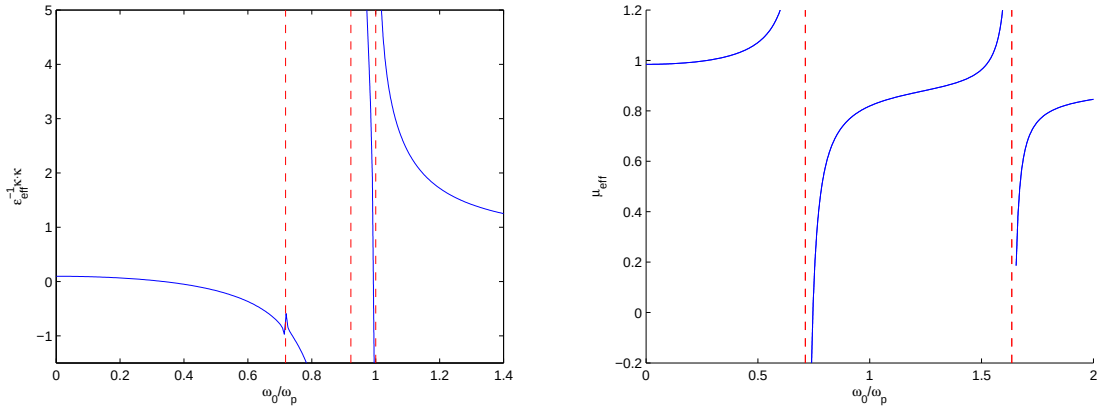

(a)

(b)

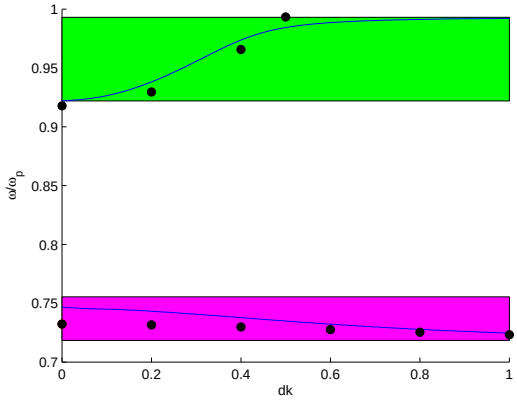

(c)

FIGURE 4.4: the case of $a = 0.2d, b = 0.4d$ and $\epsilon_R = 285$. Notice that the vertical dash lines are the asymptotes.

series (4.3.5) exhibits the precise way in which effective properties influence leading order behavior for period cells of size $d > 0$.

To verify that the leading order dispersion relation is a good predictor of the dispersive behavior of the metamaterial, we numerically compute the solutions $(\omega/\omega_p)^2$ and u^d of the nonlinear eigenvalue problem given by equation (1.2.6). These computations are carried out for different wave numbers k with propagation along the direction $(1, 0)$. The simulations are carried out using COMSOL software. Here we are interested in the range $\omega/\omega_p < 1$ for which the plasmonic material has a negative permittivity, $\epsilon_P < 0$. Two examples are considered: the first example

is the case of $a = 0.2d, b = 0.4d$ and $\epsilon_R = \epsilon_r/d^2 = 285$ and the second example is for $a = 0.15d, b = 0.4d$ and $\epsilon_R = 285$. Figure 4.4 (a)(b) (Figure4.5 (a)(b)) are the graphs of the effective properties $\epsilon_{eff}^{-1}(\frac{\omega_0}{\omega_p})\hat{\kappa} \cdot \hat{\kappa}$ and $\mu_{eff}(\frac{\omega_0}{\omega_p})$ respectively. Figure 4.4 (c) (Figure 4.5 (c)) compares the prediction given by the leading order dispersion relations $dk = \sqrt{n_{eff}^2}\frac{\omega_0}{\omega_p}$ (solid lines) with the numerical approximation of the dispersion relation given by black dots. Although the length scale of the

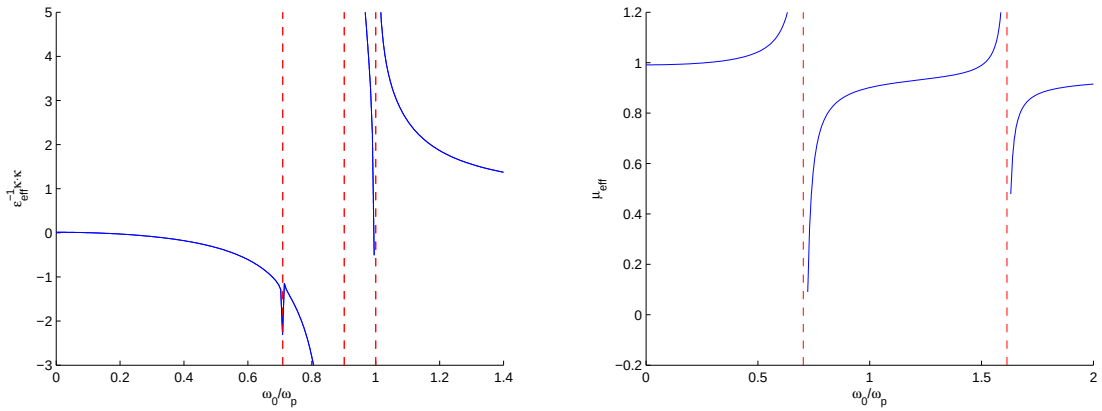

(a) (b)

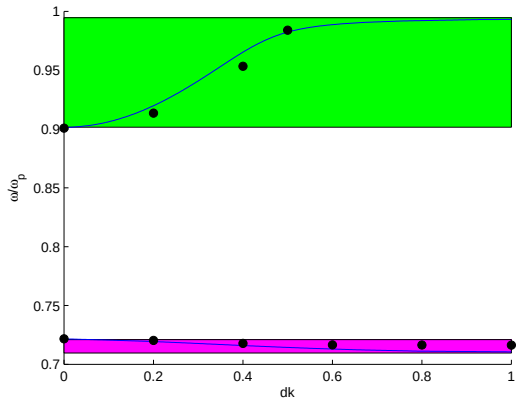

(c)

FIGURE 4.5: the case of $a = 0.15d, b = 0.4d$ and $\epsilon_R = 285$. Notice that the vertical dash lines are the asymptotes.

microstructure is not infinitesimally small compared to the radiation wavelength, the numerically calculated points (black dots) fall near the solid lines predicted by

the leading order dispersion relation. Notice that the magenta area is the prediction of the band of double negative leading order effective properties while the green area is for the double positive band. Both graphs show that the leading order dispersion relation given by the power series can well predict the Bloch wave modes in the actual crystal up to about 20% smaller than the wavelength.

References

[1] Alu, A., Engheta, N.: *Dynamical theory of artificial optical magnetism produced by rings of plasmonic nanoparticles.* Phys. Rev. B Vol 78, 085112 (2008)

[2] Adams, D.: *Sobolev Spaces.* Elsevier, Waltham(2003)

[3] Ammari, H., Kang, H. and Lee, H.: *Asymptotic analysis of high-contrast phononic crystals and a criterion for the band-gap opening.* Arch. Rational Mech. Anal. Vol 193, 679–714 (2009)

[4] Ammari, H.,Kang, H., Soussi, S. and Zribi, H.: *Layer potential techniques in spectral analysis. Part II: Sensitivity analysis of spectral properties of high contrast band-gap materials.* SIAM Multi. Model. Simu. Vol 5, 646–663 (2006)

[5] Bergman,D.J.: *The dielectric constant of a simple cubic array of identical spheres.* J. Phys. C Vol 12, 4947–4960 (1979)

[6] Bohren, C.F., Huffman, D.H.: *Absorption and Scattering of Light by Small Particles.* Wiley, Weinheim (2004)

[7] Bouchitté, G., Bourel, C. : *Homogenization of finite metallic fibers and 3D-effective permittivity tensor.* Proc. SPIE, Vol 7029, 702914 (2008)

[8] Bouchitté, G., Schweizer, B.: *Homogenization of Maxwell's equations in a split ring geometry.* SIAM Multi. Model. Simu. Vol 8(3), 717–750 (2010)

[9] Bouchitté, G. , Felbacq, D.: *Negative refraction in periodic and random photonic crystals.* New J. Phys. Vol 7, 159 (2005)

[10] Bouchitté, G. , Felbacq, D.: *Homogenization near resonances and artificial magnetism from dielectrics.* C. R. Acad. Sci. Paris I(339), 377–382 (2004)

[11] Chen, Y., Lipton, R.: *Tunable double negative band structure from non-magnetic coated rods.* New J. Phys. Vol 12, 083010 (2010)

[12] Cherdantsev, M.: *Spectral convergence for high-contrast elliptic periodic problems with a defect via homogenization.* Mathematika Vol 55, 29–57 (2009)

[13] Chern, R. L., Felbacq, D.: *Artificial magnetism and anticrossing interaction in photonic crystals and split-ring structures.* Phys. Rev. B Vol 79(7), 075118 (2009)

[14] Dolling, G., Enrich, C., Wegener, M., Soukoulis, C. M. and Linden, S.: *Low-loss negative-index metamaterial at telecommunication wavelengths.* Opt. Lett. Vol 31, 1800–1802 (2006)

[15] Felbacq, D., Bouchitté, G.: *Homogenization of wire mesh photonic crystals embdedded in a medium with a negative permeability.* Phys. Rev. Lett. Vol 94(18), 183902 (2005)

[16] Figotin, A. , Kuchment, P.: *Band-Gap Structure of the Spectrum of Periodic Dielectric and Acoustic Media. I. Scalar model.* SIAM J. Appl. Math. Vol 56(1), 68–88 (1996)

[17] Figotin, A. , Kuchment, P.: *Band-Gap Structure of the Spectrum of Periodic Dielectric and Acoustic Media. II. 2D Photonic Crystals.* SIAM J. Appl. Math. Vol 56(6), 1561–1620 (1996)

[18] Figotin, A. , Kuchment, P.: *Spectral properties of classical waves in high contrastperiodic periodic media.* SIAM J. Appl. Math. Vol 58(2), 683–702(1998)

[19] Folland , G. : *Introduction to Partial Differential Equations.* Princeton University Press, Princeton (1995)

[20] Fortes, S. P., Lipton, R. P. and Shipman, S. P.: *Sub-wavelength plasmonic crystals: dispersion relations and effective properties.* Proc. R. Soc. Lond. Ser. A Mat. doi: 10.1098/rspa.2009.0542 (2009)

[21] Fortes, S. P., Lipton, R. P. and Shipman, S. P.: *Convergent power series for fields in positive or negative high-contrast periodic media.* Comm. Partial Differential Equations Vol 36(6), 1016–1043 (2011)

[22] Hempel, R., Lienau, K.: *Spectral properties of periodic media in the large coupling limit.* Comm. Partial Differential Equations Vol 25, 1445–1470 (2000)

[23] Huangfu, J., Ran, L., Chen, H., Zhang, X., Chen, K., Grzegorczyk, T. M. and Kong, J. A.: *Experimental confirmation of negative refractive index of a metamaterial composed of Ω-like metallic patterns.* Appl. Phys. Lett. Vol 84, 1537 (2004)

[24] Huang, K. C., Povinelli, M. L. and Joannopoulos, J. D.: *Negative effective permeability in polaritonic photonic crystals.* Appl. Phys.Lett. Vol 85(4), 543 (2004)

[25] Kamotski, V., Matthies, M. and Smyshlyaev, V.: *Exponential homogenization of linear second order elliptic pdes with periodic coefficients.* SIAM J. Math. Anal. Vol 38(5), 1565–1587 (2007)

[26] Kohn, R., Shipman, S.: *Magnetism and homogenization of micro- resonators.* SIAM Multiscale Model Simul. Vol 7(1), 62–92 (2008)

[27] McPhedran, R. C., McKenzie, D.R.: *Electrostatic and optical resonances of arrays of cylinders.* Appl. Phys. Vol 23, 223–235 (1980)

[28] McPhedran, R. C., Milton, G.W. : *Bounds and exact theories for the transport properties of inhomogeneous media.* Appl. Phys. A Vol 26, 207–220 (1981)

[29] McPhedran, R. C., Nicorovici, N. A., Botten, L. C. and Movchan, A.B.: *Advances in the Rayleigh multipole method for problems in photonics and phononics.* IUTAM Symposium on Mechanical and Electromagnetic Waves in Structured Media (ed. R.C. McPhedran et al), pp. 15–28, Kluwer Academic Publishers (2001)

[30] Milton, G.W.: *Realizability of metamaterials with prescribed electric permittivity and magnetic permeability tensors.* New J. Phys. Vol 12(3), 033035 (2010)

[31] Milton, G.W.: *The Theory of Composites.* Cambridge University Press, Cambridge (2002)

[32] Nicorovici, N. A., McPhedran, R. C. and Milton, G. W.: *Transport properties of a 3 phase composite material: the square array of coated cylinders.* Proc. R. Soc. A Vol 422, 599–620 (1993)

[33] Nicorovici, N. A., McPhedran, R. C. and Milton, G. W.: *Optical and dielectric properties of partially resonant composites.* Phys. Rev. B Vol 49(12), 8479–8482 (1994)

[34] Pendry, J., Holden, A., Robbins, D. and Stewart, W.: *Low frequency plasmons in thin-wire structures.* J. Phys.: Condens. Matter Vol 10, 4785–4809 (1998)

[35] Pendry, J., Holden, A., Robbins, D. and Stewart, W.: *Magnetisim from conductors and enhanced nonlinear phenomena.* IEEE Trans. Microwave Theory Tech. Vol. 47(11), 2075–2084 (1999)

[36] Peng, L., Ran, L., Chen, H. , Zhang, H., Kong, L. A. and Grzegorczyk, T. M.: *Experimental observation of left-handed behavior in an array of standard dielectric resonators.* Phys. Rev. Lett. Vol 98, 157403 (2007)

[37] Perrins. W.T., McKenzie, D.R. and McPhedran, R.C.: *Transport properties of regular arrays of cylinders.* Pro. R. Soc. A Vol 369 207–225 (1979)

[38] Service, R. F.: *Next Wave of metamaterials hopes to fuel the revolution.* Sci. Vol 327, 138–139 (2010)

[39] Shalaev, V.: *Optical negative-index metamaterials.* Nature Photonics Vol 1, 41-48 (2007)

[40] Shalaev, V. M., Cai, W., Chettiar,U. K., Yuan, H. K., Sarychev, A. K., Drachev, V. P. and Kildishev, A. V.: *Negative index of refraction in optical metamaterials.* Opt. Lett. Vol 30, 3356–3358 (2005)

[41] Shelby, R.A., Smith D.R. and Schultz, S.: *Experimental verification of a negative index of refraction.* Sci. Vol 292, 77–79 (2010)

[42] Shipman, S.: *Power series for waves in micro-resonator arrays.* In Proceedings of the 13th International Conference on Mathematical Methods in Electrodynamic Theory, Kyiv, Ukraine: IEEE (2010)

[43] Shvets, G., Urzhumov, Y.: *Engineering the electromagnetic properties of periodic nanostructures using electrostatic resonances.* Phys. Rev. Lett. Vol 93(24), 243902-1-4 (2004)

[44] Smith, D., Padilla, W., Vier, D., Nemat-Nasser, S. and Schultz, S.: *Composite medium with simultaneously negative permeability and permittivity.* Phys. Rev. Lett. Vol 84 (18) 4184–4187 (2000)

[45] Strutt, J.W.: *On the influence of obstacles arranged in rectangular order upon the properties of a medium.* Phil. Mag. Vol 34, 481–502 (1892)

[46] Veselago, V., G.: *The electrodynamics of substances with simultaneously negative values of ϵ and μ.* Sov. Phys. Usp. Vol 10, 509 (1968)

[47] Vynck, K., Felbacq, D., Centeno, E., Cabuz, A., I., Cassagne, D. and Guizal, B.: *All-dielectric rod-type metamaterials at optical frequencies.* Phys. Rev. Lett. Vol 102, 133901 (2009)

[48] Wheeler, M. S., Aitchison, J. S. and Mojahedi, M.: *Coated non-magnetic spheres with a negative index of refraction at infrared frequencies.* Phys. Rev. B Vol 73, 045105 (2006)

[49] Yannopapas, V.: *Negative refractive index in the near-UV from Au-coated CuCl nanoparticle superlattices.* Phys. Stat. Sol. (RRL) 1(5), 208–210 (2007)

[50] Yannopapas, V.: *Artificial magnetism and negative refractive index in three-dimensional metamaterials of spherical particles at near-infrared and visible frequencies.* Appl. Phys. A Vol 87(2), 259–264 (2007)

[51] Zhang, F., Potet, S., Carbonell, J., Lheurette, E., Vanbesien, O., Zhao, X. and Lippens, D.: *Negative-zero-positive refractive index in a prism-like omega-type metamaterial.* IEEE Trans. Microw. Theory Tech. Vol 56, 2566 (2008)

[52] Zhang, S., Fan, W., Minhas, B. K., Frauenglass, A., Malloy, K. J. and Brueck, S. R. J.: *Midinfrared resonant magnetic nanostructures exhibiting a negative permeability.* Phys. Rev. Lett. Vol 94, 037402 (2005)

[53] Zhikov, V. V.: *Gaps in the spectrum of some elliptic operators in divergent form with periodic coefficients.* Algebra i Analiz Vol 16, 34-58 (2004). English translation St. Petersburg Mathematical Journal Vol 16(5), 773–790 (2005)

[54] Zhou, X., Zhao, X. P.: *Resonant condition of unitary dendritic structure with overlapping negative permittivity and permeability.* Appl. Phys. Lett. Vol 91, 181908 (2007)

Vita

Yue Chen was born on July 15 1978, in Hangzhou, Zhejiang Province, China. He finished his undergraduate studies at Shanghai University July 2001. He earned a master of science degree in mathematics from Louisiana State University in Dec. 2008. In August 2006 he came to Louisiana State University to pursue graduate studies in mathematics. He is currently a candidate for the degree of Doctor of Philosophy in mathematics, which will be awarded in August 2012.